In presenting the dissertation as a partial fulfillment of the requirements for an advanced degree from the Georgia Institute of Technology, I agree that the Library of the Institution shall make it available for inspection and circulation in accordance with its regulations governing materials of this type. I agree that permission to copy from, or to publish from, this dissertation may be granted by the professor under whose direction it was written, or, in his absence, by the dean of the Graduate Division when such copying or publication is solely for scholarly purposes and does not involve potential financial gain. It is understood that any copying from, or publication of, this dissertation which involves potential financial gain will not be allowed without written permission.

TOTAL CROSS SECTIONS FOR THE PRODUCTION OF POSITIVE IONS AND FREE ELECTRONS BY HELIUM IONS IN GASEOUS TARGETS

A THESIS

Presented to

The Faculty of the Graduate Division

by

Robert Archie Langley

In Partial Fulfillment

of the Requirements for the Degree

Doctor of Philosophy in

the School of Physics

Georgia Institute of Technology

June, 1963

5A
12T

TOTAL CROSS SECTIONS FOR THE PRODUCTION OF POSITIVE IONS AND FREE ELECTRONS BY HELIUM IONS IN GASEOUS TARGETS

Approved: _____

_____

_____

_____

Date approved by Chairman: _____

DEDICATION

This thesis is gratefully
dedicated to my wife Sara Leith
in return for her constant
encouragement and help.

ACKNOWLEDGMENTS

The successful prosecution of this work was made possible by the contributions of several people. Principal among these was Dr. D. W. Martin, who was the author's thesis advisor. His guidance was invaluable in this research. Significant contributions were also made by Dr. E. W. McDaniel, Dr. J. W. Hooper, and Dr. D. S. Harmer.

The author also expresses thanks to Mr. L. J. Puckett and Mr. J. W. Martin of the Engineering Experiment Station, who helped to operate the equipment during a portion of this work.

This research was partially supported by the Controlled Thermonuclear Branch of the U. S. Atomic Energy Commission under a contract administered by the Engineering Experiment Station of the Georgia Institute of Technology.

TABLE OF CONTENTS

TABLE OF CONTENTS (Continued)

LIST OF ILLUSTRATIONS

LIST OF ILLUSTRATIONS (Continued)

LIST OF ILLUSTRATIONS (Continued)

SUMMARY

The cross sections for the production of slow positive ions and free electrons for He^+ ions incident on helium, neon, argon, hydrogen, nitrogen, oxygen, and carbon monoxide have been measured for incident particle energies over the range from 0.133 to 1.00 MeV. Similar cross sections have been measured for He^{++} ions incident on helium and hydrogen for incident particle energies over the range from 0.50 to 1.00 MeV. Previous ionization measurements by other investigators in this field have been confined to incident particle energies below 0.18 MeV. The work reported here represents an extension of the cross sections into the energy region where the Born approximation is expected to be valid. Theoretical calculations using this approximation must be compared with experimental results in order to verify the adequacy of the wave functions of the struck atom or molecule used in the calculation.

Considering a binary or two-system collision, let us refer to one system as the target system and the other as the incident system. At the high energies of the present research generally only a small fraction of the momentum of the incident system is transferred and the incident particle suffers only a small loss of energy and emerges with only a slight deviation from its original direction of motion and therefore the identity of the incident system is well defined.

Of the several general types of elastic and inelastic processes that are possible in a binary collision, the present research is restricted to those events that produce one or more slow ions and/or free electrons.

Even with this restriction to ionization, charge transfer, and dissociation, there are still a number of distinct final states for a given pair of collision partners. Most types of experiments, however, observe all events of a certain class without distinguishing between them. If the charge state of the incident system is the same before and after the collision but the target particle is ionized we shall call the event an "ionization" event. In contrast are the "charge-changing" events in which the incident system gains or loses electrons. These include "charge-transfer" events in which the incident system takes electrons from or gives electrons to the target, and also "stripping" events in which the incident system is ionized in the collision, producing one or more free electrons. Either charge transfer or stripping events may be accompanied by ionization and/or dissociation of the target system.

For a given projectile on a given target, each class of events in general includes several distinct kinds of reactions differing in the array of slow residual particles that are produced. The energies of the latter are usually low, although a small fraction of them may have energies as high as a few hundred electron volts.

In this research, the source of energetic ions was a 1-MeV Van de Graaff positive ion accelerator, which was equipped with a beam analyzing and stabilizing system. The beam was passed through a gas cell, an electrostatic analyzer, collimating apertures, and into a collision chamber containing the target gas. The chamber dimensions and gas pressure were such that the target was "thin," in the sense that only a small fraction of the incident particles underwent any collisions at all. Electrodes parallel to the beam axis in the collision chamber collected the slow

charged residual particles produced in ionizing collisions, while the original incident particles passed through the collision volume and into a Faraday cup. Detection of both the slow and fast particles was accomplished by electrometer measurements of the electron and ion currents. A complete discussion of the design considerations and the detailed testing of the apparatus is given. Particular attention was paid to scattering of the incident beam from apertures, Faraday cup design for proper measurement of the incident beam current, the effect of background contributions and their proper assessment, target gas pressure determination, the suppression of secondary emission from the positive ion collection electrode structure, collection volume definition, collection efficiency, the effects of leakage currents, and the assessment of charge-transfer contributions.

Values for the cross sections for the production of slow positive ions and free electrons for helium ions incident on helium, neon, argon, hydrogen, nitrogen, oxygen, and carbon monoxide are presented along with data of other investigators which are available in the lower energy range.

By far the greatest uncertainty in the experiment lies in the determination of the target gas pressure, for which McLeod gauges were used. Use of a cathetometer was believed to permit a relative reading uncertainty of the 400-ml McLeod Gauge used during the He^+ measurements of less than 4 per cent in the range around 1×10^{-4} Torr. This gauge had not been absolutely calibrated, however, so that a possible error of about $\pm$ 5 per cent must be admitted in the absolute reading. This led to proportionate possible systematic error in all of the measurements, but it is emphasized that the relative values of the cross sections at various energies are not subject to this systematic error. A larger 2.2-liter McLeod Gauge, used

during the He^{++} measurements, was calibrated to an accuracy of about ± 1 per cent while deviation of any one pressure reading from an average of about five readings was as high as ± 5 per cent. This error was due to sticking of the mercury column in the capillary and was believed to be random.

The absolute error brackets for the cross sections involving He^{+} ions are about ± 8 per cent for σ_{+} and about ± 11 per cent for σ_{-}, while the relative accuracies of the cross sections with respect to each other are about ± 5 per cent. The absolute error brackets for the cross sections involving He^{++} ions are about ± 7 per cent for σ_{+} and about ± 10 per cent for σ_{-}, while the relative accuracies are about ± 5 per cent.

For most of the cross sections measured it was possible to estimate the cross section for simple ionization using values of "charge-changing" and "stripping" cross sections obtained by Pivovar et al. Theoretical calculations for ionization cross sections using the Born approximation have been made by Mapleton (He^{++} + He) and Bates and Griffing (He^{++} + H) for point-charge ions, i.e., completely stripped nuclei, and were found to agree well with the present results. A theoretical treatment of He^{+} incident on atomic hydrogen has been made by Boyd et al. and Bates and Griffing. A doubling of the theoretically determined atomic ionization cross section to obtain the molecular cross section is suspect in that it leads to a cross section higher than the experimentally observed cross section. A scaling procedure used for point-charge ions was applied to the theoretical calculations and agreement between the estimated experimental ionization cross section and the scaled theoretical cross section was excellent.

A general theoretical treatment of high energy ionization by Bethe for incident point-charge ions was compared with the data for He^{++} incident on both helium and hydrogen. Known experimental proton ionization cross sections were used to determine empirically certain needed constants in this theory. The agreement between this theory and present results is good. Also the estimated experimental ionization cross sections of several gases by He^{+} ions were compared with Bethe's calculations to examine the proposition that the Bethe results could be used for the case of an ion carrying bound electrons by using an "effective" charge Z_i lying between the nuclear charge and the actual net charge of the ion. To be a useful concept, the effective charge for a given incident ion must be found to be independent of the target gas and of the incident ion energy. The theoretical calculations referred to here describe only "simple" ionization events in which the incident ion does not gain or lose electrons. Therefore the present experimental data on the total ion and electron production by He^{+} had to be corrected for the appreciable contributions from charge-changing events encountered at high energies. It was found that the estimated cross section for simple ionization was greater than that for incident protons of the same velocity by a factor that was very nearly independent of energy above 0.6 MeV, and varied only from 1.3 to 1.5 for the four gases hydrogen, helium, argon, and nitrogen. Thus the concept of an effective charge of about 1.2e for He^{+} does seem to have at least a qualitative validity. It is noteworthy that this value is appreciably less than the effective charge 1.69e deduced in variation calculations of the ground state wave functions of helium. This difference is not unexpected since the two cases are quite different, and may be most sensitive to quite different spatial regions of the wave function.

CHAPTER I

INTRODUCTION

The field of atomic collisions is of basic interest since the nature of the interactions between atoms and molecules can be investigated through observations of collision phenomena. In principle, quantum mechanical calculations could be made for any atomic collision process if a complete set of wave functions for the partners in a collision were known. However, wave functions adequate to describe collision phenomena are not known at the present time except for hydrogenic atoms and ions. Detailed theoretical calculations have not been made except for the simplest cases, i.e., those involving electrons, protons, neutral hydrogen atoms, and singly and doubly charged helium ions as projectiles incident on targets of atomic hydrogen, helium, and lithium. Even for most of these simple cases the calculations were difficult and involved approximations whose validity is difficult to assess except by resort to comparison with experimental results. The calculations are particularly sensitive to the form of the wave functions at large radius. In contrast, most calculations involving properties of bound states, from which most of the existing detailed knowledge of wave functions is drawn, are not particularly sensitive to the details in this region.

Most of the existing calculations for ionization processes at high energies have been made in the Born approximation, which is expected to be valid only for high relative impact energies. In the present research

experimental observations have been extended to sufficiently high energies that the results provide a check of the validity of the assumptions made in both existing and future calculations. The comparison between theory and experiment will therefore yield information about atomic and molecular wave functions, especially at large radius.

Earlier experimental work on atomic ionization processes has been confined to lower energy regions, and until recently most practical interest in such collisions has been confined to similar energies. Recent developments in the field of high temperature plasma physics have engendered a renewed interest in basic data on all kinds of collision phenomena at higher energies. A major difficulty in attaining a very hot plasma is "cooling" of the ions in the plasma by collisions with contaminants in the system. Among the approaches to the problem of controlled thermonuclear reactions there are several schemes which utilize high energy injection, and knowledge of the ionization cross sections for various projectiles moving at high velocities through various target gases should prove of value.

Other areas in which high energy ionization processes are of interest include astrophysics, the physics of the upper atmosphere, and the technology of various types of detection devices in high energy nuclear physics.

Chapter II contains a discussion of some of the more pertinent terms used in the field of high energy atomic collisions, a statement of the purpose of the experiment reported in this thesis, a list of pertinent review articles dealing with the field of atomic collisions, and a discussion of some existing theories of binary collisions.

Chapter III deals specifically with phenomena related to the passage of helium ions through a gas. A cross-section notation is discussed and applied to the collision of singly-charged helium ions incident on molecular hydrogen. Particular theoretical calculations dealing with incident helium ions are discussed, with a method through which theory and experiment may be compared.

The experimental equipment and method is discussed in Chapter IV. Chapter V contains discussions of data corrections, comparison of present results with other experimental investigations, and errors. In Chapter VI available theoretical calculations are compared with the present experimental results.

CHAPTER II

DEFINITIONS AND THEORETICAL BACKGROUND

This chapter contains a discussion of some of the terms used in the field of high energy atomic collisions, a statement of the purpose of the experiment reported in this thesis, a list of pertinent review articles dealing with the field of atomic collisions, and a discussion of some existing theories of binary collisions.

A number of types of events may occur when atomic or molecular systems collide. There may be simple elastic scattering, where momentum is transferred but the internal structures of both systems remain unchanged. Other events classified as inelastic may involve electron transfer between the two systems, or excitation, ionization or dissociation of one or both of the colliding systems. Elastic scattering, excitation and simple dissociation events will not be further considered here.

Considering a binary or two-system collision, let us refer to one system as the target system and the other as the incident system. At the high energies of the present research generally only a small fraction of the momentum of the incident system is transferred. The incident particle suffers only a small loss of energy and emerges with only a slight deviation from its original direction of motion, so that the identity of the incident system is well defined.

Even with the restriction to ionization, charge transfer, and dissociation, there are still a number of distinct final states for a given pair of collision partners. Most types of experiments, however, observe

all events of a certain class without distinguishing between them. If the charge state of the incident system is the same before and after the collision but the target particle is ionized we shall call the event an "ionization" event. In contrast are the "charge-changing" events in which the incident system gains or loses electrons. These include "charge-transfer" events in which the incident system takes electrons from or gives electrons to the target, and also "stripping" events in which the incident system is ionized in the collision, producing one or more free electrons. Either charge-transfer or stripping events may be accompanied by ionization and/or dissociation of the target system.

In order to study collision reactions in detail, it is necessary to be able to express the probability of a given reaction as a quantitative measure. This quantity must be one that may be measured experimentally and calculated theoretically so that experimental and theoretical values can be compared. The concept of collision cross section is frequently used (see Appendix). This concept permits the assignment of a hypothetical size, which is related to the probability of occurrence of a specific event, to the target systems.

Most present experimental observations have fallen into two distinct classes: the "thick" target approach in which the incident particle beam passes through a sufficient quantity of target material to attain a statistical charge state equilibrium and the "thin" target approach in which the probability of multiple collisions by a single incident system is negligible. Most charge-changing collision experiments have involved thick targets and observations on the emerging fast particles. In contrast, most of the ionization measurements have been thin target experiments and have involved observation of the residual slow particles.

The purpose of the experiment reported in this thesis is to measure the total cross sections for the production of positive ions and free electrons in gaseous targets by helium ions in the energy range 0.133-1.00 MeV. The target gases are helium, neon, argon, hydrogen, nitrogen, oxygen, and carbon monoxide. The "thin" target method is used. The total cross sections for the production of positive ions and free electrons involve the sum of the apparent ionization cross section and certain charge-changing cross sections. The apparent ionization cross section, as defined by Massey and Burhop,[1] is the cross section for single ionization plus twice the cross section for double ionization plus three times the cross section for triple ionization, etc. With respect to the slow ions, only the total current is observed and it has not been ascertained directly what fraction of this current is due to multiply charged ions or what part is due to events in which the charge state of the incident ion is changed.

Previous work with incident helium ions has dealt primarily with ionization cross sections at lower energies and with charge-changing cross sections at both high and low energies.

Experimental work prior to 1951 has been thoroughly surveyed by Massey and Burhop.[1] Reviews of the charge-transfer field prior to 1957 by Allison are pertinent.[2,3] A recent article by Federenko reviews ionization reactions.[4] A work soon to be published by McDaniel reviews the field of atomic collisions.[5]

A discussion is presented on some of the existing theories pertinent to this research. The range of energies in this research is such that the range of impact velocities is large compared with the velocities of orbital atomic electrons, but small compared with the velocity of light, i.e.,

$10^8 < v < 5 \times 10^9$ cm/sec. In general, the partners in a collision have internal structure, i.e., nucleus plus electrons, so that the collision process is essentially an interaction involving many particles. It is necessary to reduce this many body problem to a binary collision problem in order to use one of the formulations which have been devised to deal with binary collisions. Some of these binary collision formulations are presented below.

Partial Waves[6]

The method of partial waves was devised to deal with collision problems which involve spherically symmetric interaction potentials. In the space-time representation of scattering, the incident particle beam is considered as a plane wave incident on a scattering center. The scattered wave is expanded as an infinite series of spherical harmonics with each term multiplied by an appropriate radial wave function. Each term in this expansion is called a "partial wave." As a result of the interaction with the scattering center each scattered wave is shifted in phase from that which it would have had if the scattering center had not been there. The cross section for a particular reaction is given by an infinite sum in which each term involves a function of one of the phase shifts. The cross section may then be found if all the phase shifts are known. In order to calculate these phase shifts one must essentially solve the Schrödinger equation, however.

This method is most useful if the series converges rapidly enough so that only a few phase shifts need be calculated. The number of phase shifts that will influence the cross section in any given case can be obtained from the equation

$$\ell(\ell+1) = k^2 r_o^2 \qquad (2\text{-}1)$$

where ℓ is the number of phase shifts that must be calculated, k is the wave number of the incident wave, and r_o is the radius beyond which the scattering potential has become negligible.

This method is used with short range potentials such as those encountered in nuclear physics. The high energy of the incident particles used in this experiment and the long range scattering potential involved render this method impracticable because of the large number of phase shifts that must be calculated, but it is used at much lower energies to calculate elastic scattering and charge-transfer cross sections for atomic systems.

Born and Distorted Wave Approximations[6]

The time-independent Schrödinger wave equation for a binary collision in which the collision partners have internal structure is

$$\left[-\frac{\hbar^2}{2m}\nabla_r^2 + T_A(\bar{r}_A) + T_B(\bar{r}_B) + V_A(\bar{r}_A) + V_B(\bar{r}_B) + V(\bar{r},\bar{r}_A,\bar{r}_B)\right]\psi(\bar{r}_A,\bar{r}_B,\bar{r}) = E\psi \qquad (2\text{-}2)$$

where the atomic systems are denoted by A and B. In Equation (2-2), T_A and T_B are respectively the kinetic energy operators for systems A and B, and V_A, V_B are their internal potential energies. To obtain an approximation to ψ suitable for the determination of cross sections, it is usual to expand ψ in the form

$$\psi(\bar{r}_A,\bar{r}_B,\bar{r}) = \sum_n \varphi_{An}(\bar{r}_A)\,\varphi_{Bn}(\bar{r}_B)\,\psi_n(\bar{r}) \qquad (2\text{-}3)$$

where φ_{An} and φ_{Bn} are the wave functions describing the internal states of A and B and $\psi_n(\bar{r})$ describes the relative motion in state n. Using the relations

$$[T_A + V_A - E_{An}]\, \varphi_{An} = 0 \tag{2-4}$$

$$[T_B + V_B - E_{Bn}]\, \varphi_{Bn} = 0 \tag{2-5}$$

$$\frac{2m}{\hbar^2}\,[E_{An} + E_{Bn} - E_{Ao} - E_{Bo}] = k_o^2 - k_n^2 \tag{2-6}$$

and multiplying Equation (2-2) through by $\varphi^*_{An}\,\varphi^*_{Bn}$ and integrating over $\bar{r}_A$ and $\bar{r}_B$ leads to the infinite set of coupled differential equations for ψ_n

$$(\nabla_r^2 + k_n^2)\,\psi_n(\bar{r}) = \sum_m U_{nm}\,\psi_m(\bar{r}) \tag{2-7}$$

where

$$U_{nm} = \frac{2m}{\hbar^2}\int \varphi^*_{An}(\bar{r}_A)\,\varphi^*_{Bn}(\bar{r}_B)\,V(\bar{r}_A,\bar{r}_B,\bar{r})\,\varphi_{Am}(\bar{r}_A)\,\varphi_{Bm}(\bar{r}_B)\,d\bar{r}_A d\bar{r}_B \tag{2-8}$$

The summation sign is meant to include integration over states of positive energy as well as bound states of the atoms A and B. Solutions of these equations are required to be well-behaved functions with asymptotic form

$$\psi_n \sim \frac{f_n(\theta,\varphi)}{r}\, e^{i\bar{k}_n\cdot\bar{r}} + e^{i\bar{k}_o\cdot\bar{r}}\,\delta_{on} \tag{2-9}$$

The differential cross section for inelastic scattering in which the system goes from state o to state n is then

$$I_{on}(\theta,\varphi)\, d\Omega = \frac{v_n}{v_o} |f_n(\theta,\varphi)|^2\, d\Omega \qquad (2\text{-}10)$$

with v_o and v_n the velocities of relative motion in the two states. The differential cross section for elastic scattering is

$$I_{oo}(\theta,\varphi)\, d\Omega = |f_o(\theta,\varphi)|^2\, d\Omega \qquad (2\text{-}11)$$

A major difficulty is to obtain a complete orthogonal set of wave functions φ_{An} and/or φ_{Bn} which must be known in order to obtain Equation (2-7). The set of wave functions must contain bound state and continuum state wave functions. A complete set of exact wave functions is actually known only for one atom, the hydrogen atom. In all other cases they must be approximated. Most theoretical calculations to date have assumed the validity of Equation (2-7) even though the explicit wave functions subsequently used in the computation are not truly orthogonal. Unfortunately it is very difficult to reach any a priori conclusion as to the extent of the inaccuracy in the results caused by this approximation. Only by comparison with experimental results can any conclusions be reached.

Born's approximation considers the interaction between the colliding systems as a small perturbation to the total Hamiltonian of the system. This results in putting all terms other than the matrix element associated with the incident wave equal to zero so that Equation (2-7) becomes the single equation

$$(\nabla_r^2 + k_n^2)\, \psi_n(\bar{r}) = U_{no}\, e^{i\bar{k}_o \cdot \bar{r}} \qquad (2\text{-}12)$$

Using the Green's function

$$G(r,r_1) = -\frac{1}{4\pi}\frac{e^{\pm ik_n|\bar{r}-\bar{r}_1|}}{|\bar{r}-r_1|} \tag{2-13}$$

one obtains the solution with the asymptotic form of Equation (2-10) as

$$\psi_n(r) = +\delta_{on}\, e^{i\bar{k}_o\cdot\bar{r}} - \frac{1}{4\pi}\int U_{no}(\bar{r}_1)\,\frac{e^{i\bar{k}_o\cdot\bar{r}_1}\, e^{ik_n|\bar{r}-\bar{r}_1|}}{|\bar{r}-\bar{r}_1|}\, d\bar{r}_1 \tag{2-14}$$

This method of calculation has been used to calculate ionization cross sections for a bare nucleus and for a bare nucleus plus one (1s) electron incident on atomic hydrogen and helium for the case that $\frac{k^2h^2}{2m} >> E_o$, where E_o is the internal energy of the struck atom.

A less drastic approximation is the distorted wave approximation. For this one assumes that transitions through intermediate states may be ignored so that only the matrix elements $U_{no}(=U_{on})$, U_{nn} and U_{oo} are considered, then the set of coupled Equations (2-7) become

$$(\nabla_r^2 + k_n^2 - U_{nn})\,\psi_n(\bar{r}) = U_{no}\,\psi_o(\bar{r}) \tag{2-15}$$

$$(\nabla_r^2 + k_o^2 - U_{oo})\,\psi_o(\bar{r}) = U_{on}\,\psi_n(\bar{r}) \tag{2-16}$$

An additional approximation may be made if U_{no} is small by putting the right hand side of Equation (2-16) equal to zero. This method has been used for atomic processes at low relative energy for which the Born approximation becomes inadequate.

The formulation presented here must be altered in order to deal with identical particles, but this presents only more numerical difficulty.

The Classical Approach of Gryzinski[7]

Gryzinski has given a classical theory of atomic cillisions in which he assumes that elastic scattering, ionization, excitation, and other inelastic interactions between charged particles and atoms can be described by a Coulombic type interaction between the incident ion and the atomic electrons, treated classically, and depend on the atomic electron's binding energy and momentum distribution treated quantum mechanically.

Gryzinski used the results of Chandrasekhar[8,9] in which the energy transfer between two colliding free particles moving arbitrarily with respect to each other and interacting through an inverse square force was calculated classically in terms of general kinematical parameters describing the collision.

Gryzinski has integrated Chandrasekhar's results over distributions of the collision parameters appropriate to the impact of fast ions on electrons orbiting about a fixed target atom to obtain $\sigma(\Delta E,\theta)$, the classical cross section for scattering of an incident particle in direction θ with change of energy ΔE. He has further obtained $\sigma(\Delta E)$, the classical cross section for the incident particle to have an energy change ΔE, without regard to θ.

The cross section for a collision with energy loss greater than U is

$$Q(U) = \int_{U}^{\Delta E_{max}} \sigma(\Delta E)\, d(\Delta E) \qquad (2\text{-}17)$$

and similarly the cross section for an encounter with loss of energy in the interval $U_1 \leq \Delta E \leq U_2$ is

$$Q(U_2;U_1) = \int_{U_1}^{U_2} \sigma(\Delta E)\, d(\Delta E) \tag{2-18}$$

Gryzinski asserts that the cross section for ionization of an atom is given simply by the classical cross section for transfer to the atomic electron, treated as a free particle but with a speed distribution appropriate to its bound initial state, of energy at least as great as the ionization potential. Thus the ionization cross section for an atom is

$$Q_j^{atom} = \sum_i \int_o^\infty N^i(v_e)\, Q(U_j^{(i)})\, dv_e \tag{2-19}$$

where $N^i(v_e)$ is the velocity distribution of i shell electrons of the atom and $U_j^{(i)}$ is their ionization potential. For the simplest case, $N^i(v_e)$ is approximated by the single velocity obtained from the expectation value of the electron kinetic energy appropriate to electrons in the i shell.

Similarly, the cross section for excitation of the atom to the level n is represented as the classical cross section for transfer of energy at least as great as the excitation energy of level n but less than the excitation energy of any higher level. Thus the cross section for the excitation of the level n is

$$Q_{exc}^n = \sum_i \int_o^\infty N^{(i)}(v_e)\, Q(U_{n+1}^{(i)} ; U_n^{(i)})\, dv_e \tag{2-20}$$

where $U_n^{(i)}$ and $U_{n+1}^{(i)}$ are the excitation energies of the levels n and n + 1 respectively from the shell i.

Quantal effects are thus considered only indirectly, by restricting the energy transfer to the electron to values compatible with the fact that it is bound in a quantized state, and by the use of an initial speed distribution for the electrons deduced from the quantum mechanical description of the initial state.

Agreement between this theory and experimental results for inelastically scattered electrons from molecular hydrogen is very good for the total cross section although it is relatively inaccurate for describing the angular distributions.[10,11] Agreement is excellent for ionization cross sections of hydrogen and helium by electrons. In light of some of the assumptions made the agreement between this theory and experiment is rather surprising.

CHAPTER III

PHENOMENA RELATED TO THE PASSAGE OF HELIUM IONS THROUGH A GAS

This chapter deals specifically with phenomena related to the passage of helium ions through a gas. To illustrate the multiplicity of possible events, a list of reactions for the case of fast singly-charged helium ions incident on molecular hydrogen is presented. A cross section notation is discussed and applied to these reactions. Definitions of total production cross sections and some charge-changing cross sections are given. Cross-correlation between the two types of cross sections are discussed. Particular theoretical calculations using the Born approximation are discussed, and a method is presented by which theory and experiment may be compared.

A list of reactions for the case of fast singly-charged helium ions incident on molecular hydrogen is presented below. The first symbol appearing on the left and right hand side of each equation denotes the fast incident particle before and after the collision, respectively. This particle may or may not experience a change in its charge state as the result of the reaction, but in any event theory and experiment show that most of the time it retains essentially all of its initial energy and its original direction of motion if the velocity of relative motion is large compared to the atomic orbital electron velocity, as was the case for this experiment. The second symbol on the left hand side of the equation denotes the target particle before the collision. The remaining terms on the right hand side

represent the fragments of the target particle after collision plus any free electrons stripped from the incident projectile.

$$He^{+} + H_2^{\circ} \rightarrow He^{+} + H_2^{+} + e \qquad {}_{10}\sigma^{i}_{11} \qquad (3\text{-}1)$$

$$He^{+} + H^{+} + H^{\circ} + e \qquad {}_{10}\sigma^{id}_{11} \qquad (3\text{-}2)$$

$$He^{+} + H^{+} + H^{+} + 2e \qquad {}_{10}\sigma^{id}_{12} \qquad (3\text{-}3)$$

$$He^{+} + H^{+} + H^{-} \qquad {}_{10}\sigma^{id}_{10} \qquad (3\text{-}4)$$

$$He^{\circ} + H_2^{+} \qquad {}_{10}\sigma^{c}_{01} \qquad (3\text{-}5)$$

$$He^{\circ} + H^{+} + H^{\circ} \qquad {}_{10}\sigma^{cd}_{01} \qquad (3\text{-}6)$$

$$He^{\circ} + H^{+} + H^{+} + e \qquad {}_{10}\sigma^{cid}_{02} \qquad (3\text{-}7)$$

$$He^{++} + H_2^{\circ} + e \qquad {}_{10}\sigma^{s}_{20} \qquad (3\text{-}8)$$

$$He^{++} + H^{\circ} + H^{\circ} + e \qquad {}_{10}\sigma^{sd}_{20} \qquad (3\text{-}9)$$

$$He^{++} + H_2^{+} + 2e \qquad {}_{10}\sigma^{si}_{21} \qquad (3\text{-}10)$$

$$He^{++} + H^{+} + H^{\circ} + 2e \qquad {}_{10}\sigma^{sid}_{21} \qquad (3\text{-}11)$$

$$He^{++} + H^{+} + H^{+} + 3e \qquad {}_{10}\sigma^{sid}_{22} \qquad (3\text{-}12)$$

$$He^{++} + H_2^{-} \qquad {}_{10}\sigma^{c}_{2\bar{1}} \qquad (3\text{-}13)$$

$$He^{++} + H^{-} + H^{\circ} \qquad {}_{10}\sigma^{cd}_{2\bar{1}} \qquad (3\text{-}14)$$

$$He^{++} + H^{+} + H^{-} + e \qquad {}_{10}\sigma^{cid}_{20} \text{ or } {}_{10}\sigma^{sid}_{20} \qquad (3\text{-}15)$$

Reaction (3-1) is the simple ionization collision, while Reaction (3-5) is the simple charge-transfer event, and Reaction (3-8) is the simple stripping reaction. Reactions (3-5) through (3-15) are charge-changing collisions.

The same information contained in each reaction equation may be conveyed by use of a generalization of a cross section representation introduced by Hasted.[12] We shall let ${}_{ab}\sigma_{mn}$ represent the cross section for the reaction in which a and m are the initial and final charges respectively of the fast incident particle, while b and n are the initial and final charges respectively of the target particle. A superscript c, i, d, or s indicates charge transfer, ionization, dissociation, and stripping, respectively. In the preceding list of reactions the cross section representing each reaction is given following it.

As has been stated in Chapter I, a given experiment measures the sum of some group of the individual cross sections. The cross sections measured in this research are denoted by σ_+ and σ_-, where σ_+ represents the total cross section for the production of slow positive ions and σ_- represents the total cross section for the production of free electrons and negative ions. These cross sections may be represented for the collision of He^+ on H_2 as follows:

$$\sigma_+ = \left[{}_{10}\sigma^{i}_{11} + {}_{10}\sigma^{id}_{11} + 2\,{}_{10}\sigma^{id}_{12} + {}_{10}\sigma^{id}_{10}\right] + \left[{}_{10}\sigma^{c}_{01} + {}_{10}\sigma^{cd}_{01} + 2\,{}_{10}\sigma^{cid}_{02}\right] \qquad (3\text{-}16)$$

$$+ \left[{}_{10}\sigma^{si}_{21} + {}_{10}\sigma^{sid}_{21} + 2\,{}_{10}\sigma^{sid}_{22} + {}_{10}\sigma^{cid}_{20}\right]$$

and

$$\sigma_- = \left[{}_{10}\sigma^{i}_{11} + {}_{10}\sigma^{id}_{11} + 2\,{}_{10}\sigma^{id}_{12} + {}_{10}\sigma^{id}_{10}\right] + \left[{}_{10}\sigma^{cid}_{02}\right] + \left[{}_{10}\sigma^{s}_{20}\right. \tag{3-17}$$

$$\left. + {}_{10}\sigma^{sd}_{20} + 2\,{}_{10}\sigma^{si}_{21} + 2\,{}_{10}\sigma^{sid}_{21} + 3\,{}_{10}\sigma^{sid}_{22} + {}_{10}\sigma^{c}_{2\bar{1}} + {}_{10}\sigma^{cd}_{2\bar{1}} + 2\,{}_{10}\sigma^{cid}_{20}\right]$$

It is now evident that what has been measured in this research is the weighted sum of individual cross sections. In a "thin" target experiment these cross sections are calculated from the relations

$$\sigma_+ = (I^+/I_i)(1/n\ell)\ \text{cm}^2/\text{molecule} \tag{3-18}$$

$$\sigma_- = (I^-/I_i)(1/n\ell)\ \text{cm}^2/\text{molecule} \tag{3-19}$$

where I^+ and I^- are the positive and negative currents collected from a collision region of length ℓ by traverse electric fields, n is the number density of gas molecules in the collision chamber, and I_i is the incident ion current. These expressions are developed in the Appendix.

The cross sections for the incident He^+ ion to pick up an electron or be stripped of its electron are denoted by σ_{10} and σ_{12}, respectively, where the first figure in the subscript represents the charge state of the incident ion before collision and the second its charge state after collision. These cross sections, written in terms of the individual cross sections (3-1) through (3-15) for He^+ incident on hydrogen, are:

$$\sigma_{10} = {}_{10}\sigma^{c}_{01} + {}_{10}\sigma^{cd}_{01} + {}_{10}\sigma^{cid}_{02} \tag{3-20}$$

and

$$\sigma_{12} = {}_{10}\sigma^{s}_{20} + {}_{10}\sigma^{sd}_{20} + {}_{10}\sigma^{si}_{21} + {}_{10}\sigma^{sid}_{21} + {}_{10}\sigma^{sid}_{22} + {}_{10}\sigma^{c}_{2\bar{1}} + {}_{10}\sigma^{cd}_{2\bar{1}} + {}_{10}\sigma^{cid}_{20} \tag{3-21}$$

It is true in general that for singly-charged helium ions incident on any gas that the difference between σ_+ and σ_- is the same as the difference between σ_{10} and σ_{12}. A check of the present measurements against charge-transfer experiment measurements may therefore be made.

For four of the gases studied the cross sections σ_{10} and σ_{12} have been measured previously over at least part of the energy range of this experiment. The experimental technique used in the measurement of σ_{10} and σ_{12} is the measurement first of the ratio of the two cross sections by a thick target beam equilibrium method and second the measurement of one of them by a beam attenuation method.[2]

The gross apparent ionization cross section σ_i is the quantity which may be directly compared with existing theoretical and experimental data and is defined as the cross section for single ionization plus twice the cross section for double ionization plus three times the cross section for triple ionization, etc. It is therefore necessary to reduce σ_+ and σ_- to σ_i. This cross section for the specific reaction of He^+ incident on H_2 is given by:

$$\sigma_i = {}_{10}\sigma_{11}^{i} + {}_{10}\sigma_{11}^{id} + 2\,{}_{10}\sigma_{12}^{id} + {}_{10}\sigma_{10}^{id} \tag{3-22}$$

$$= \sigma_+ - \sigma_{10} - \sigma_{12} - {}_{10}\sigma_{02}^{cid} - {}_{10}\sigma_{22}^{sid} + {}_{10}\sigma_{20}^{s} + {}_{10}\sigma_{20}^{sd} \tag{3-23}$$
$$+ {}_{10}\sigma_{2\bar{1}}^{c} + {}_{10}\sigma_{2\bar{1}}^{cd}$$

$$= \sigma_- - 2\,\sigma_{12} - {}_{10}\sigma_{02}^{cid} - {}_{10}\sigma_{22}^{sid} + {}_{10}\sigma_{20}^{s} + {}_{10}\sigma_{20}^{sd} + {}_{10}\sigma_{2\bar{1}}^{c} \tag{3-24}$$
$$+ {}_{10}\sigma_{2\bar{1}}^{cd}$$

Although the values of σ_+, σ_-, σ_{10}, and σ_{12} have been determined experimentally for several of the gases studied, the cross sections for the individual reactions are not known at present, therefore reasonable estimates must be made in order to find an approximate σ_i.

Not all atomic systems form negative ions, but those that do usually form then with low binding energy. It is expected that if the collision is hard enough to strip the bound electron from the incident helium ion then it is probable that no negative ion will be formed. This assumption cannot be proved at present, but it may possibly be justified by the fact that some of the cross sections involving formation of negative ions have been measured at much lower energies than the present experiment and have generally been found to fall off rapidly with increasing energy. All cross sections involving the formation of negative ions will be considered negligible.

It will be convenient to define a quantity "a" as the ratio to σ_{12} of the cross section for simple stripping events including dissociation of molecular targets.

For the particular reaction of He^+ incident on hydrogen

$$a = \frac{{}_{10}\sigma^{s}_{20} + {}_{10}\sigma^{sd}_{20}}{\sigma_{12}} \tag{3-25}$$

and

$$\sigma_i = \sigma_+ - (\sigma_{10} + \sigma_{12}) + a\,\sigma_{12} - {}_{10}\sigma^{cid}_{02} - {}_{10}\sigma^{sid}_{22} \tag{3-26}$$

$$= \sigma_- - 2\,\sigma_{12} + a\,\sigma_{12} - {}_{10}\sigma^{cid}_{02} - {}_{10}\sigma^{sid}_{22} \tag{3-27}$$

It is argued that "a" is small, for if the collision is "hard" enough to strip the bound electron from the incident helium ion then it is highly probable that the target system will also be ionized. The ionization potential of the electron of He^+ is 54.4 volts and the ionization potentials of the outer electrons of all target gases studied in this research are less than 25 volts. It is then assumed that "a" is equal to zero. The remaining individual cross sections in Equations (3-26) and (3-27) represent complex events and it seems quite likely that they are improbable and contribute in only a minor fashion. Therefore the apparent ionization cross section for incident He^+ projectiles on the target gases were obtained by the relations

$$\sigma_i \simeq \sigma_+ - (\sigma_{10} + \sigma_{12}) \tag{3-28}$$

$$\simeq \sigma_- - 2\,\sigma_{12} \tag{3-29}$$

For completeness it is necessary to examine here the process used for obtaining σ_i from σ_+ and σ_- for incident He^{++} projectiles on various target gases. The apparent cross section for ionization is given by

$$\sigma_i = \sigma_+ - \sigma_{21} - \sigma_{20} + x \tag{3-30}$$

$$= \sigma_- + x \tag{3-31}$$

where x represents a complex reaction and will be assumed small and set equal to zero. It is also seen that $\sigma_+ - \sigma_- = \sigma_{21} + \sigma_{20}$ with no approximations.

Theoretical calculations pertinent to this research have been made for a bare nucleus and for a bare nucleus plus one electron incident on atomic hydrogen and helium.

Bare Nucleus Incident On Hydrogen

Bates and Griffing[13] have calculated the cross section for the atomic process

$$x^{Ze} + H^{o}(1s) \rightarrow X^{Ze} + H^{+} + e \qquad (3\text{-}32)$$

using the Born approximation. A method of obtaining an approximate gross apparent ionization cross section for the molecular process has been indicated in reference 13. Although the results calculated for Equation (3-32) were presented only in graphical form rather than in explicit analytic form, the following generalization was made:

If a fast point charge of charge Z_b collides with a nucleus to which one electron is bound in the 1s state, then the cross section for removal of that electron takes the general form (Equation 21 of Reference 13):

$$\sigma_i = \left(\frac{Z_b}{\Delta E}\right)^2 f\left(\frac{M\Delta E}{E}\right) \qquad (3\text{-}33)$$

in which:

ΔE is the ionization energy for removal of the electron,

M is the reduced mass of the colliding system,

E is the kinetic energy of the relative motion,

f is a function of unspecified analytic form.

This formula permits scaling of the graphical results given for Reaction (3-33) to any other reaction that meets the above description.

It has often been assumed that a hydrogen molecule is simply equivalent in an energetic collision process to two independent hydrogen atoms, so that the molecular cross section would be expected to be simply twice

the atomic cross section. However, in Equation (3-33) there is an explicit dependence on the ionization energy ΔE of the electron to be removed. The vertical ionization energy of one electron in the hydrogen molecule is appreciably different from the atomic ionization energy, being, in fact, greater by the factor 1.2.

The scaling procedure followed was this: The molecule was considered to be equivalent to two free neutral atoms in every respect except that account was taken of the fact that the ionization energy is 1.2 times the normal atomic value. Ignored were the effects of the second atom on the reduced mass of the system consisting of the projectile and the first atom, on the ratio of the incident particle energy to the relative motion energy, and of course on the form of the electronic wave function that was used in the calculation of the atomic cross section. To this approximation, a theoretical cross section for the removal of one electron from the molecule by the impact of an incident point charge of energy E will be twice the given atomic cross section for the incident point charge energy $E/1.2$, divided by $(1.2)^2$. This cross section should actually correspond to the sum of the cross sections for all of the several kinds of molecular ionization events, since the theoretical treatment made no restrictions on the final state of the molecule, and so the result should include all possible final states. Therefore, this cross section should correspond to the approximated gross experimental ionization cross section.

Bare Nucleus Incident on Helium

Theoretical calculations in the Born approximation of the cross sections for ionization and simultaneous ionization and excitation of

helium by a point charge have been made by Mapleton.[14] He assumed that the helium electronic wave functions may be approximated by products of normalized hydrogen wave functions in which the helium nucleus had an effective charge Z_1 of 1.6875 for the ground state. He examined three cases corresponding to various choices for Z_2, the effective charge associated with the Coulomb field acting on the final state bound electron, and Z_3, the effective charge associated with the Coulomb field acting on the final state positive energy electron. These cases were:

Case I:	$Z_2 = 2$,	$Z_3 = 1$
Case II:	$Z_2 = 2$,	$Z_3 = Z_1$
Case III:	$Z_3 = Z_1$	for the $\ell = 0$ term of the wave function of the final state positive energy electron
	$Z_3 = 1$	for the $\ell > 0$ terms of the wave functions of the final state positive energy electron.

Mapleton has pointed out that the cross sections determined from calculations based on the assumptions of Case III would be expected to be the most realistic.

Ionization cross sections for He^{++} ion impact and electron impact on helium have been calculated by Erskine[15] through an application of the Born approximation.

The foregoing calculations imply that the ionization cross section for incident He^{++} ions should be four times the cross section for incident protons of the same velocity.

Bare Nucleus Plus One Electron Incident On Hydrogen

The gross ionization cross section for the reaction:

$$Y_{(1s)}^{(Z-1)e} + H(1s) \rightarrow Y_{(1s)}^{(Z-1)e} + H^{+} + e \qquad (3\text{-}34)$$

where Y represents an ion or atom consisting of a bare nucleus plus one electron in the 1s electronic state, having net charge (Z-1)e, has been calculated theoretically.[13,16] Again if a comparison between the present experiment and theory is to be made the cross sections for the atomic process must be scaled in order to obtain the cross sections for the molecular process. The earlier scaling procedure cannot obviously be easily applied for this case because the theoretical cross section is given by a sum of terms where the individual terms were not known. Boyd et al.[16] have suggested only that comparison between theory and molecular experimental results be made by regarding each molecule as two atoms, therefore just doubling the atomic cross section. Such a procedure would ignore the fact that the binding energy of the electron in the molecule is greater than it is in the atom. Application of the procedure described in the section "Bare Nucleus Incident On Hydrogen" to take account of the difference cannot be justified on the basis of any equations displayed in References 13 or 16. However, such a procedure was applied to this case, and the result was found to be in very good agreement with experimental results.

CHAPTER IV

EXPERIMENTAL EQUIPMENT AND METHOD

The objective of this research was the measurement of the cross section for the production of slow positive ions and free electrons for helium ions incident on helium, neon, argon, hydrogen, nitrogen, oxygen, and carbon monoxide. The energy of the incident particles ranged from 0.133-1.00 MeV.

The source of the energetic protons was a 1-MeV Van de Graaff positive ion accelerator, which was equipped with a beam analyzing and stabilizing system. The beam was passed through differentially pumped collimating apertures into a collision chamber containing the target gas. The chamber dimensions and gas pressure were such that the target was "thin," in the sense that only a small fraction of the incident particles underwent any ion-producing collisions at all. Electrodes parallel to the beam axis in the collision chamber collected the slow charged particles produced in ionizing collisions, while the original incident particles passed through the collision volume and into a Faraday cup. Detection of both the slow and fast particles was accomplished by simultaneous electrometer measurements of the electron, ion, and the incident beam current.

A schematic drawing of the apparatus is given in Figure 1. Following is a point by point discussion of the more important features of the apparatus, considered in sequence from the ion source to the electrometer circuits.

The Incident Beam Source

The ion source of the Van de Graaff had two gas inlet lines, each equipped with a thermomechanical leak. The two gases used in the ion source were molecular hydrogen and helium. The ion source, which is a RF excited source, provided ample beams of H^+ ions and He^+ ions but produced essentially no yield of He^{++} ions. The time required to switch from one beam to another was a matter of a few minutes.

The beam from the Van de Graaff entered the apparatus at the left hand side of Figure 1. It was then deflected through 90° in the analyzing magnet, which assured that it consisted essentially only of the desired ions. The beam ion energy was stabilized by electronic regulation of the accelerator voltage to maintain equal currents on the two stabilizer slit edges, which amounted to demanding a constant deflection in the regulated magnetic field. (This was the standard stabilizing system provided by the accelerator manufacturer, the High Voltage Engineering Corporation. The nominal energy spread was ± 2 kev at 1 MeV.) Thus the particle energy was determined by the value of the magnetic field and was measured by measuring that field. Employed for this purpose was a Harvey Wells model G-501 nuclear magnetic resonance gaussmeter, which as used had relative and absolute accuracies of one part in 10^3. The deflection geometry was calibrated empirically by measuring the magnetic field corresponding to the 1.019-MeV threshold of the nuclear reaction $H^3(p,n)He^3$, using a tritium-zirconium target.

Gas Cell

Since the ion source of the Van de Graaff provided only a minimal He^{++} beam, it was necessary to use the He^+ beam from the Van de Graaff

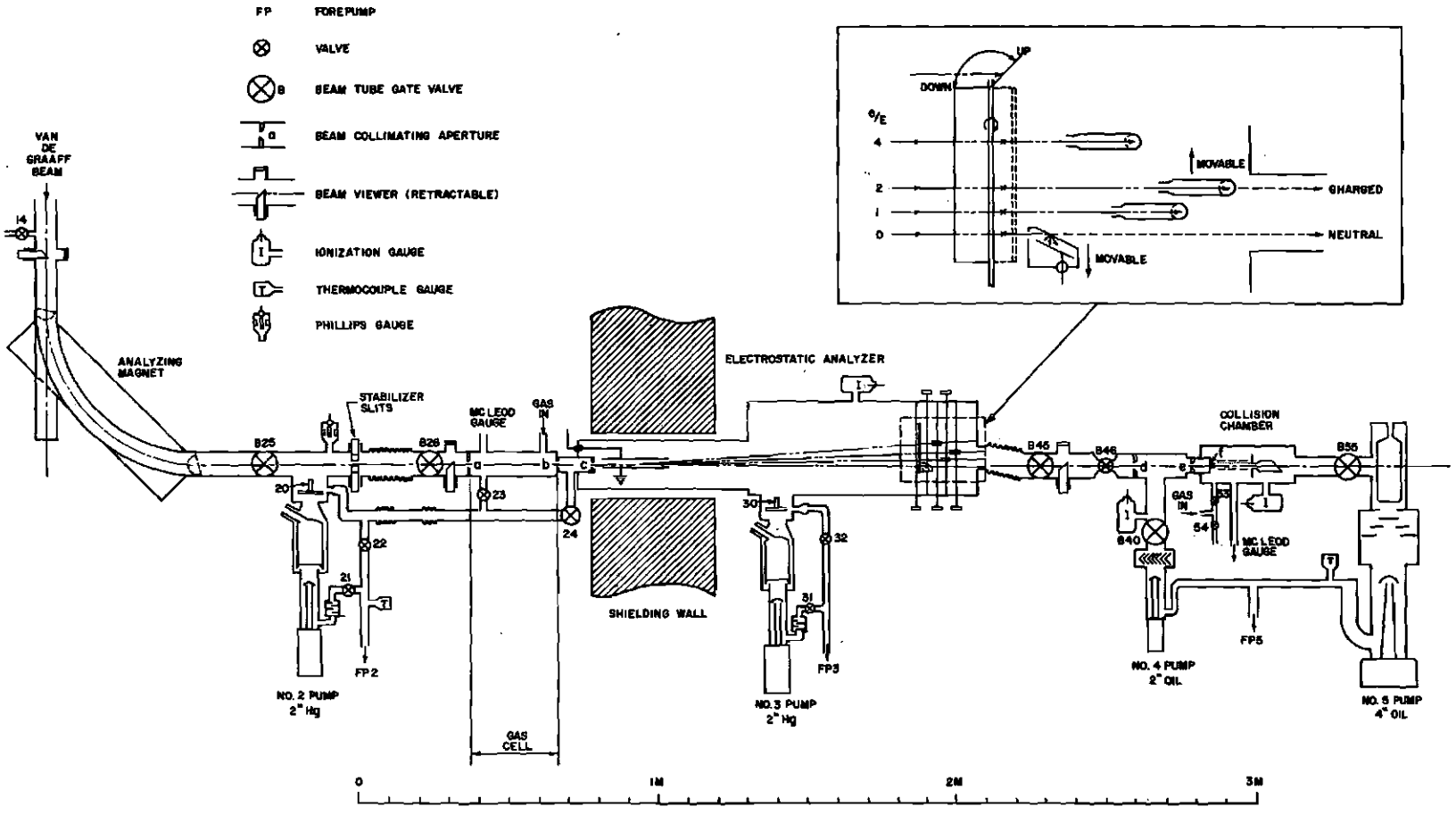

Figure 1. Schematic View of Apparatus.

accelerator to obtain an He^{++} beam. This was accomplished by passing the He^{+} beam through a gas cell which contained argon gas at pressures which ranged from 1.0 to 7.0 x 10^{-3} Torr. The He^{+} beam underwent charge-changing collisions so that the beam leaving the gas cell consisted of He^{0}, He^{+}, and He^{++}.

The apertures "a" and "b" of Figure 1 define the length of the gas cell. These apertures were round and knife-edged with a diameter of 1/16 inch. They were machined through 1/4-inch-thick brass plates which, except for the apertures, formed essentially vacuum-tight closures of the beam tube. With this arrangement, the pressure in the accelerator vacuum system remained within tolerable bounds only when the pressure in the gas cell remained below 7 x 10^{-3} Torr.

Gas entered the cell continually through a variable leak and was pumped continually through the apertures "a" and "b." The valve 23 of Figure 1 permitted the gas cell to be pumped to pressures of approximately 3 x 10^{-6} Torr with the gas inlet closed. Valve 23 was normally closed when working with the He^{++} beam. The pressure in the gas cell was measured with a McLeod gauge.

A differentially pumped vestibule was provided following the gas cell and is indicated in Figure 1. The pumping provided on this chamber sufficed to allow the pressure beyond aperture "c" to be kept below 2 x 10^{-5} Torr with gas present in the gas cell at the maximum working pressure. Aperture "c" was round and knife-edged and was machined through a 1/4-inch brass plate, which except for the aperture was essentially a vacuum-tight closure of the beam tube. The aperture had a diameter of 3/32 inch.

Electrostatic Analyzer Section

Following the gas cell, the beam enters the electrostatic analyzer, which selects from the mixed beam those particles which happen to be in the desired charge state. For clarity the electrostatic analyzer section and the collision chamber are shown rotated 90° about the beam axis into plane view in Figure 1. Thus the beam deflections produced by the analyzer are actually in the horizontal plane, rather than verticle as they appear in the figure. The analyzer consists of two parallel plates 17 cm long and 1.2 cm apart, to which a variable potential difference of up to 5000 volts may be applied. This potential difference was maintained by a Hamner High Voltage Power Supply Model N-413. With the "normal" operating voltage of 2400 volts applied to the plates, the three components of a 1-MeV helium beam (He^{o}, He^{+}, and He^{++}) are separated by about 2 centimeters at the exit end of the analyzer section. The deflection plates are mounted on a holder which could be rotated about the beam axis from an external control, permitting adjustment of the plane of the deflected beams to coincide with the horizontal plane of the beam detectors and the exit port. The gas cell with its apertures and the deflector assembly are so constructed that they could be rigidly assembled and aligned optically before they were installed in the vacuum housing of the analyzer section.

Provision was made for monitoring the intensities of all of the separated components of the beam. Near the exit end of the analyzer section are three small Faraday cups and a secondary-emission neutral detector. Each unit has a lead screw by means of which it can be independently positioned horizontally to collect one of the separated component beams. A frosted glass "viewer" plate in the same region can be rotated into

position to intercept all of the beams, providing a visual indication of the beam locations by means of the fluorescence of the glass. The arrangement is shown in the insert in Figure 1, and Figure 2 is a close-up photograph of this portion of the apparatus. The detector corresponding to the component beam being used for cross section measurements can be moved aside by means of its lead screw, as is indicated in Figure 1, permitting that beam to pass out through the exit port, while the other detectors remain in position to monitor the remaining components.

The collision chamber and its entrance collimator are constructed as a rigid assembly that connects to the analyzer section through a flexible bellows. This whole assembly can be moved horizontally relative to the analyzer to align it at will with any of the three beam positions that fall within the analyzer exit port (charge-energy ratio, $e/E = 0$, 1, or 2; see Figure 1). In Figure 1 the collision chamber is shown aligned with the undeflected neutral beam. For the He^{++} measurements the chamber is placed in line with the $e/E = 2$ position. Figure 3 is a photograph of the portion of the apparatus to the right of the shielding wall in Figure 1, viewed from the opposite side. The mechanical arrangements provided for the horizontal movements of the collision chamber can be seen as well as a jackscrew arrangement provided in the supports to facilitate vertical alignment adjustments. In Figure 3 the collision chamber is shown offset toward the camera to align with the $e/E = 2$ beam position for He^{++} measurements.

When the apparatus is aligned as described for He^{++} measurements, application of the "normal" 2400 volts to the deflector plates directs 1.0 MeV He^{++} ions into the collision chamber along the $e/E = 2$ trajectory,

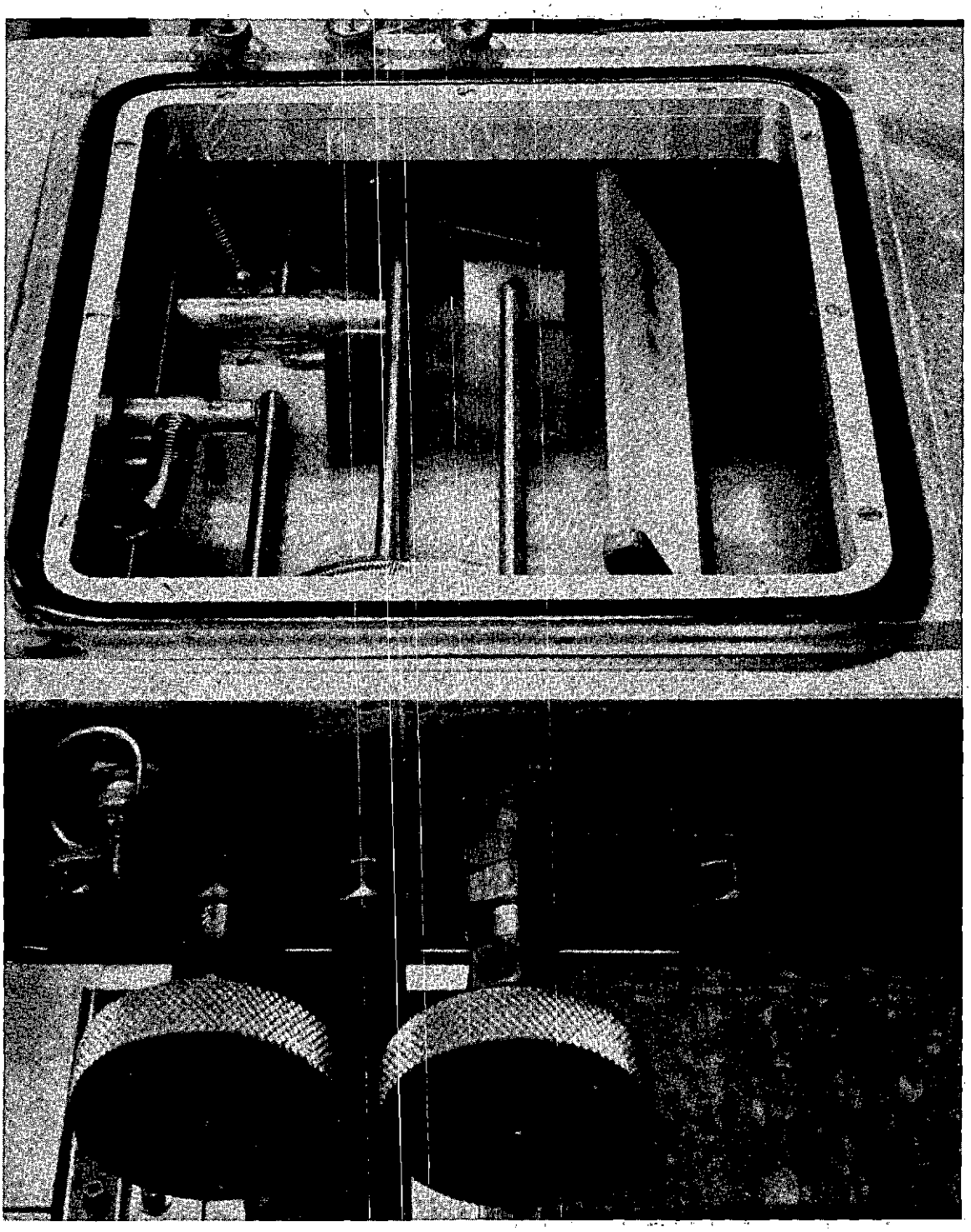

Figure 2. Interior View of Electrostatic Analyzer with Faraday Cups.

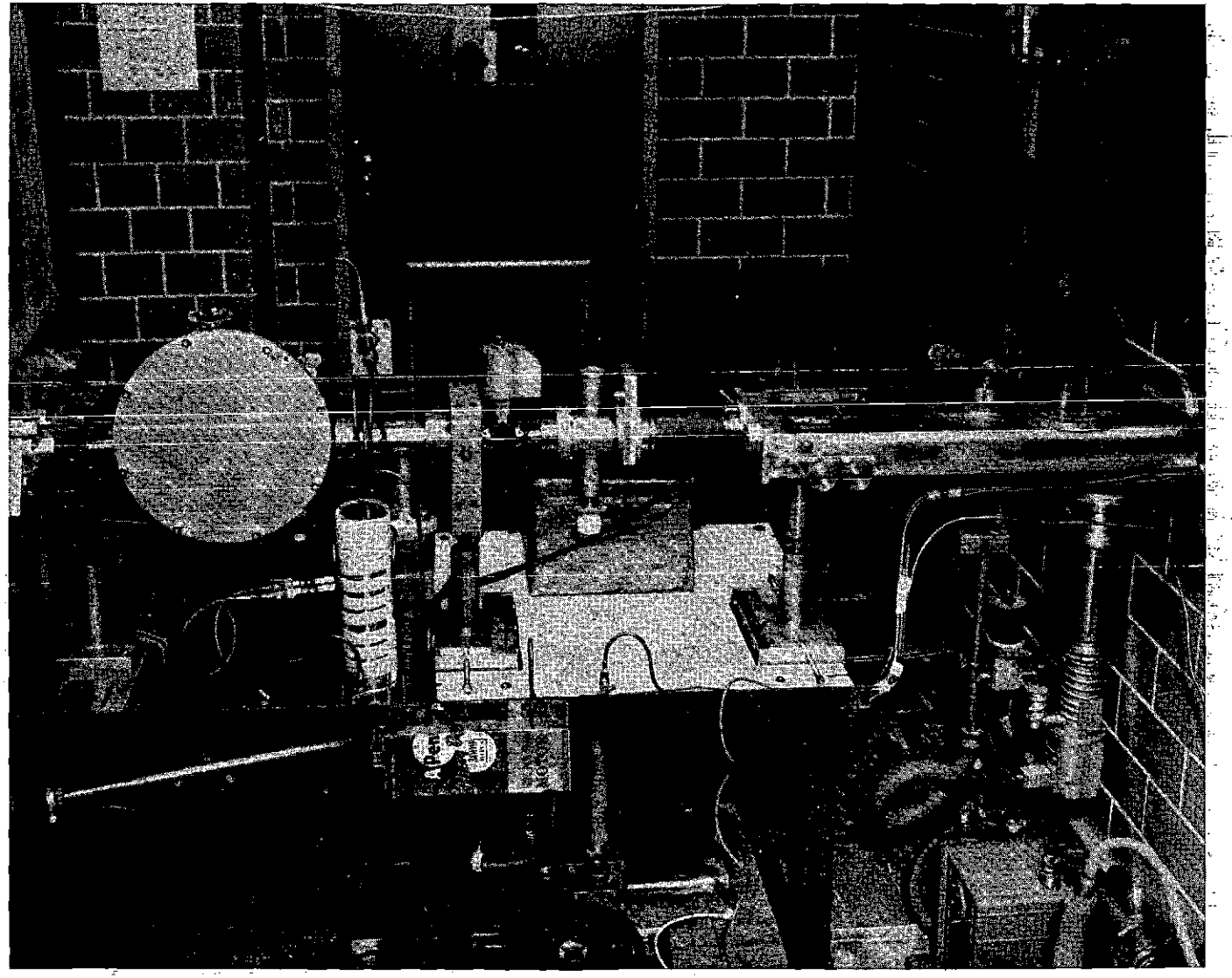

Figure 3. Exterior View of Electrostatic Analyzer and Collison Chamber.

while the He^{+} component is monitored by the Faraday cup at e/E = 1. By simply doubling the voltage, one can direct the He^{+} beam into the chamber, while collecting and monitoring the He^{++} component at the e/E = 4 position. In addition, the ion-source gas supply in the Van de Graaff can be readily switched from helium to hydrogen so that with only a readjustment of the field of the analyzing magnet, a beam of 1.0 MeV protons can also be directed into the chamber along e/E = 2 by the double voltage. Thus the He^{++} measurements were readily checked against well established H^{+} and He^{+} results without disturbing the mechanical alignment of the apparatus. This feature proved to be extremely valuable in establishing confidence in the measurements.

With the present arrangement, a He^{++} beam of satisfactory intensity can be obtained throughout the energy range from 1.0 MeV down to about 0.5 MeV, below which the yield falls very rapidly. The range could be extended downward somewhat if pressures greater than 7×10^{-3} Torr could be used in the gas cell. Unfortunately the presently available pumping speed on the small chamber between "b" and "c" (Figure 1) has proved to be inadequate to permit such pressures without a prohibitive increase in the pressure in the analyzer section. The criterion for the maximum pressure tolerable in this region is that recontamination of the separated He^{++} beam by further charge-changing collisions between the deflector plates and the first slit of the collision chamber entrance collimator ("d" in Figure 1) shall not exceed 1 per cent. Since the "electron pick-up" cross sections for He^{++} increase rapidly with decreasing energy, the maximum-pressure criterion rapidly becomes more stringent in this direction, so that the minimum energy attainable with only a 1 per cent beam contamination is

0.50 MeV. The maximum permissible pressure versus beam energy is presented in Figure 4.

The pressure in the analyzer section was read with a Veeco type RG-75 Ionization Gauge. Since the nominal calibration of the ionization gauge is for nitrogen, each pressure reading was corrected for argon, since this was the gas used in the gas cell.

The Collision Chamber and Its Associated Differentially Pumped Collimator

For reference in the following discussion collimating apertures are designated by the letters with which they are labeled in Figures 1 and 5. Aperture designs and pumping speeds were chosen so that the greatest part of the pressure drop from the target region would occur at "f," so that the effective beginning of the flight path in the target gas began there. The total path length from there to the entrance of the Faraday cup was about 5 inches. Apertures "d" and "e" each have circular knife-edged openings 1/16-inch in diameter, and the minimum opening in "f" is a knife-edged hole slightly over 3/32-inch in diameter. Thus the collimation of the beam was defined by "d" and "e," and only a few scattered particles impinged on the edge of "f." The opening in "f" presented a small solid angle to the secondaries produced at "e," and very few should have passed through. However, as noted above, "f" is designed to have a relatively large pumping impedance, while the thin plate containing "e" is perforated with three large off-center holes to present a small pumping impedance.

As is indicated in Figure 5 the portion of the apparatus that contains the three apertures "d," "e," and "f" can be rigidly assembled before insertion into the collision chamber, so that all three apertures could be

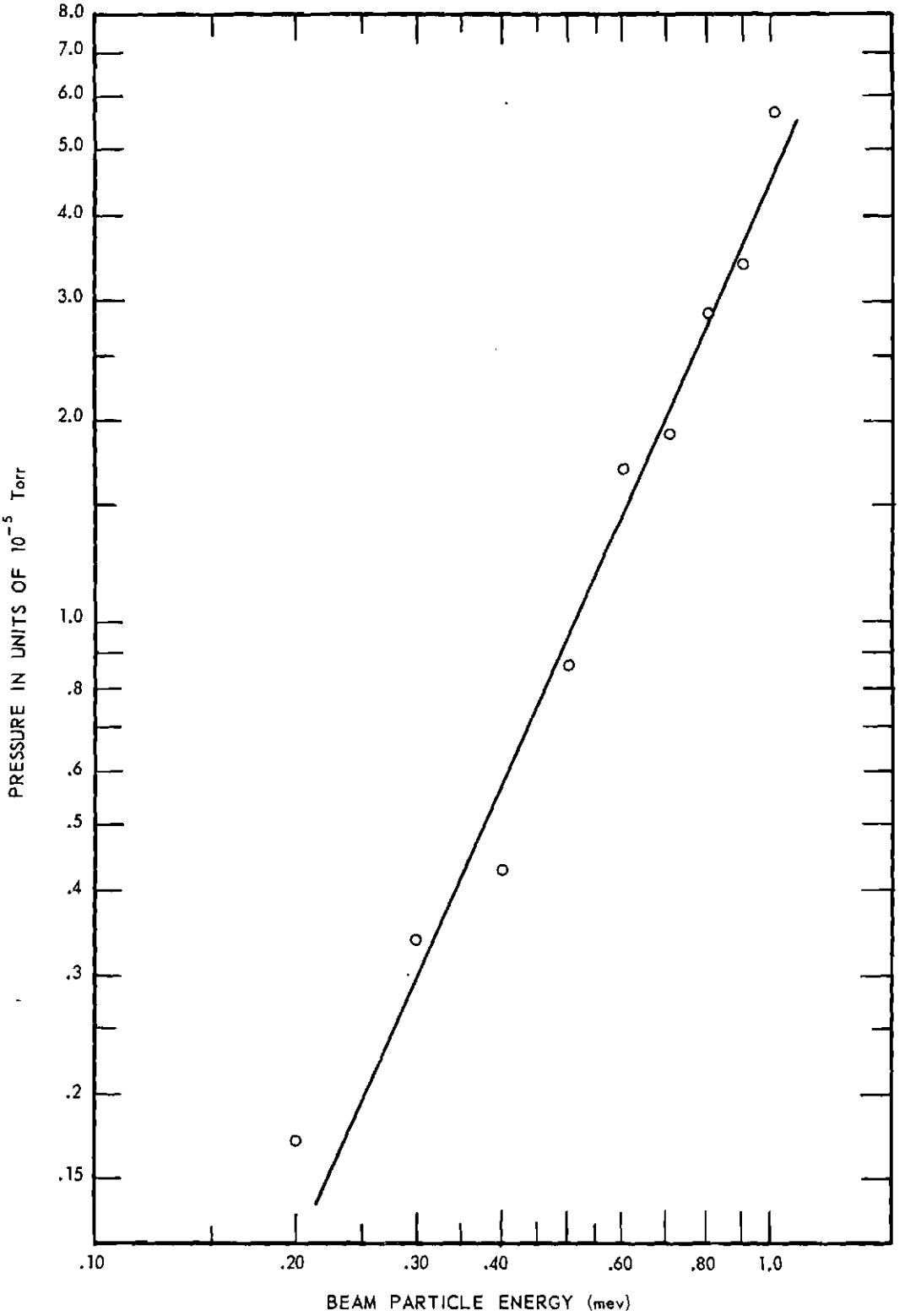

Figure 4. Maximum Permissible Pressure in Electrostatic analyzer Section for One Per Cent He^{++} Beam Contamination.

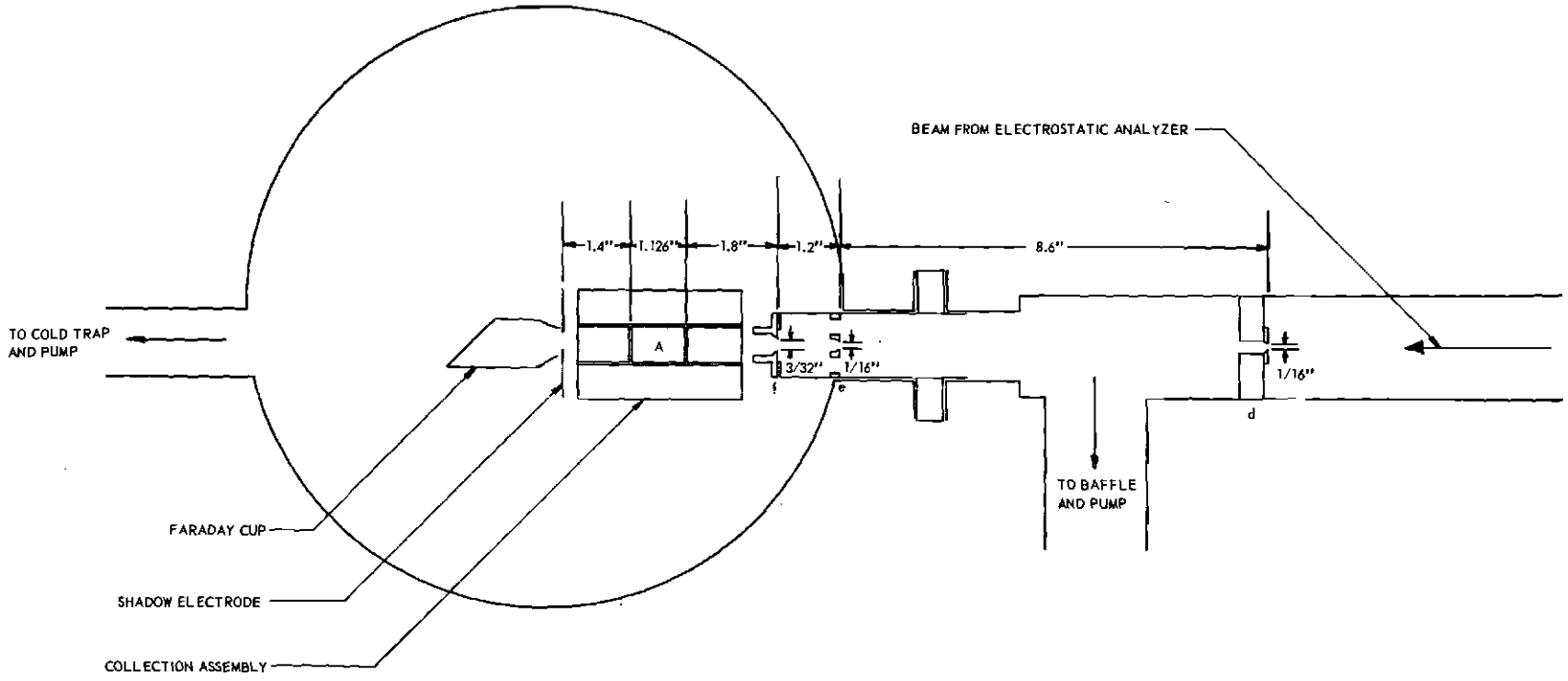

Figure 5. Schematic View of Collison Chamber.

accurately aligned optically. The pumping between apertures "d" and "f" was provided by a two-inch oil diffusion pump topped by a water-cooled baffle.

A photograph of the open collision chamber is shown in Figure 6. The collimated beam entered from the right and passed between the two electrode assemblies and into a Faraday cup. Electrical connections from the electrodes passed to the outside through seven kovar-glass seals in the rear wall of the chamber. The chamber was evacuated by the four-inch baffled and trapped oil diffusion pump at the left. A one-quart Stanley stainless steel vacuum bottle was installed between the pump and the valve to serve as a liquid nitrogen cold trap. An ionization vacuum gauge was attached to the chamber at a hole visible in the lower part of the chamber. The pressure could not be monitored continuously because the ionization gauge could not be left on while any ionization currents were being measured because electrons were "sucked" from the gauge on to the collection plates. A cold-trapped McLeod gauge was connected to a hole, hidden by the electrode assemblies, that looked directly into the space between the assemblies. A CEC GM-100 McLeod Gauge was used as the absolute pressure measuring device during the early part of these measurements involving incident He^{+} ions while a more sensitive CEC GM-110 McLeod Gauge was used during the measurements involving He^{++} ions. Each McLeod gauge was read with a cathetometer. Target gases were admitted through a mechanical leak after being passed through a cold trap.

The gate valve B55 of Figure 1 could be used as a throttling valve to permit higher gas pressures in the collision chamber without an excessive gas throughput, which might give rise to pressure gradients in the

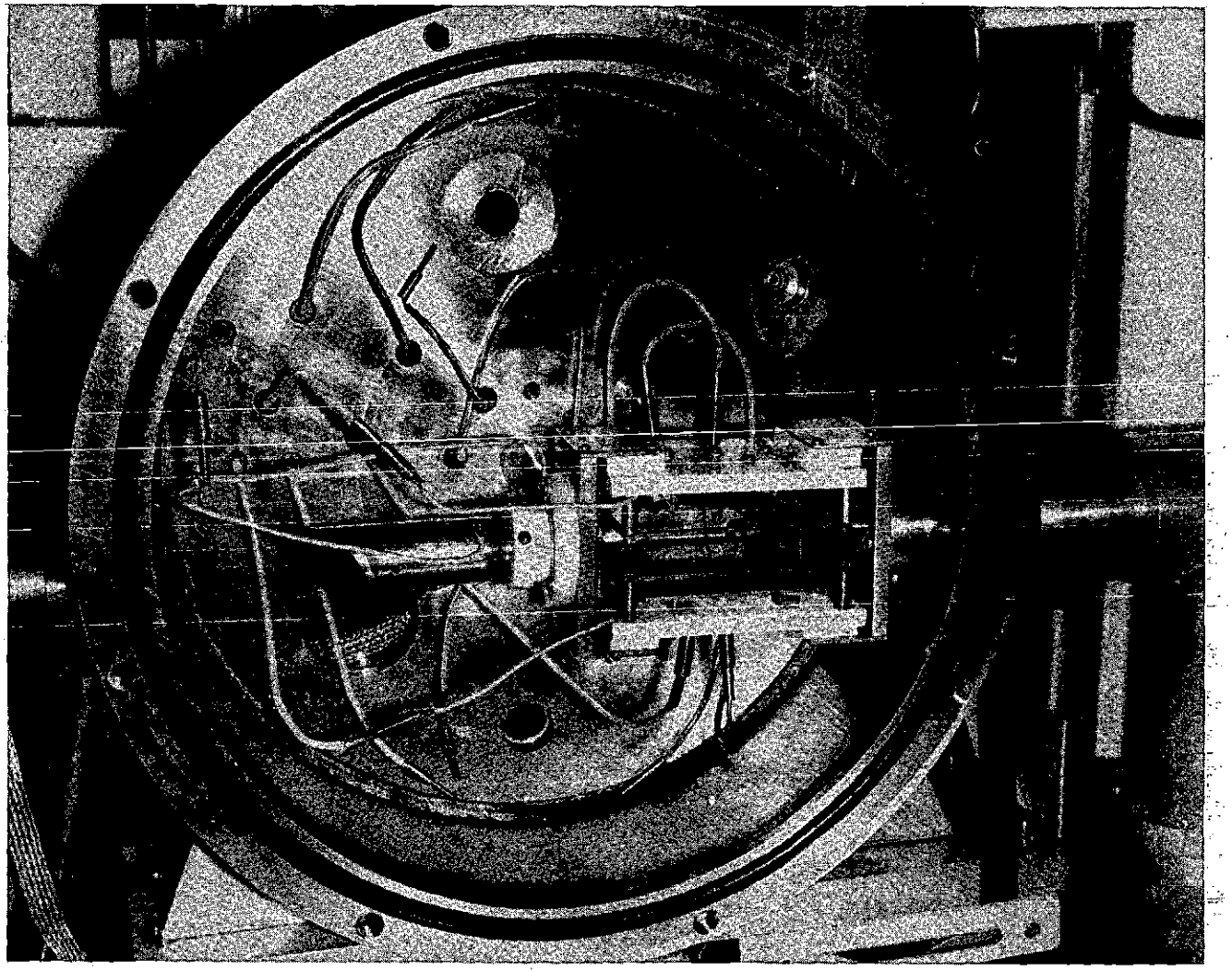

Figure 6. Interior View of Collison Chamber.

collision chamber and consequent uncertainties in the effective gas density in the collision region. Tests were made to insure that there were no gradients. The four-inch diffusion pump was operated continuously, even during a run when the target gas was in the chamber at the working pressure. The constriction was adjusted so that the resulting throughput of gas did not exceed the capabilities of the associated forepump. Working pressure was maintained by a continuous input of fresh target gas and was varied throughout the working range from 0.5 to 10.0 x 10^{-4} Torr simply by adjusting the input rate. The purpose of this constant pumping was to keep the impurity level in the chamber essentially constant, independent of the working gas pressure. Thus the ionization currents due to impurities arising from outgassing of interior surfaces and back diffusion of pump oil vapor, which were measured with no target gas input, could be subtracted directly from all the readings with target gas present. In the course of all the measurements this "background gas" correction ordinarily amounted to only 5 to 10 per cent. The ultimate pressure in the chamber, obtained by closing the gas inlet, was too small to be read meaningfully with the McLeod gauge. It was measured by the ionization gauge to have an average value of almost 3 x 10^{-6} Torr, using the gauge manufacturer's nominal calibration for nitrogen. This was assumed to give only the general order of magnitude, however, since the composition of the background was unknown.

The target gas pressures ranged from 1.0 to 10.0 x 10^{-4} Torr for He^{+} ions incident on helium and hydrogen, the gases with the smallest cross sections. For the other gases the upper limit on the highest pressure was less because the cross sections were correspondingly larger. With the installation of the more sensitive McLeod gauge the pressure could be read

accurately to lower pressures and the pressure range for the measurements involving He^{++} ions incident on helium and hydrogen was 0.5 to 5.0 x 10^{-4} Torr.

Measurement of the Incident Beam Intensity I_i

Two different Faraday cups were used at different times to collect the incident ions after they had traversed the collision volume. One was a bottled-shaped copper cup whose diameter was smallest at the open neck. The 1/2-inch inside diameter of the neck subtended an angle of 6.5° at the entrance aperture, "f," and about twice that angle at a point on the beam axis at the center of the effective collision volume. The second was a deep copper cylinder having an entrance aperture of 1/2-inch and containing a wad of steel wool to serve as "electron velvet," that is, an essentially "black" absorber for the ion beam and the secondary electrons it produces. The second cup was installed midway in the measurements to deal with what appeared to be difficulties with secondary electrons and/or X-ray photons generated by impact of the beam within the cup. Both theoretical and experimental evidence indicated that only a few of the fast incident ions that have a collision would scatter more than a few degrees. With the "thin target" gas density used in these experiments, fewer than 4 per cent of the incident ions underwent any sort of ion-producing collisions, and the number undergoing large angle elastic scattering collisions should have been negligible. It was expected that far less than 1 per cent of all incident particles would fail to enter the collection cup.

A disk-shaped "shadow" electrode with a sharp-edged circular aperture just smaller than the inside diameter of the mouth of the cup was

located immediately in front of the cup and intercepted those few particles which had scattered through an angle so large that they would not have entered the cup. If not stopped, such particles might have struck the outside of the cup and released secondary electrons, resulting in a false increase in the apparent collected current. This "shadow" electrode was held at a negative potential with respect to the Faraday cup to suppress the escape of secondary electrons from the interior of the cup. It was found that a suppression voltage of 20 to 67-1/2 volts was sufficient to produce saturation in the measured value of the incident current. The convenient value of 67-1/2 volts was used throughout the measurements.

The Collector Assemblies and Electrometers

Preliminary measurement of the cross sections σ_+ and σ_- were made for He^+ on the target gases hydrogen and helium using the apparatus described in the thesis of J. W. Hooper.[17] The cross sections for the other target gases were about an order of magnitude larger than those for hydrogen and helium and could not be measured using this collection assembly while keeping thin target conditions without going to impracticably low target gas pressures. The above mentioned collection assembly was miniaturized to reduce the length of the flight path of the incident beam in the target gas. The cross sections σ_+ and σ_- for He^+ ions on the target gases hydrogen and helium were remeasured using the miniaturized collection assembly. The results obtained with the miniaturzied structure agreed quite well with those gotten using the larger structure after certain problems were solved.

The miniaturized collector assembly is described below. A diagram of one of the slow-particle collector assemblies is shown in Figures 5 and 8.

The collector plate had five segments, each separately mounted to the rigid 1/2-inch teflon backing, with its front surface 1/4-inch in front of the backing. The center segment was cut to an accurate length of 1.106 ± 0.001 inches in the beam direction, and all segments were accurately spaced 0.010 inch apart. All five sections were always held at the same potential, so that the field in front of the assembly was essentially the same as if it had been one large continuous plate. However, only the ion (or electron) currents collected by the center segment was ever included in the electrometer circuit for measurement. The remaining segments served as guards to assure that the field in front of the active segments was parallel and uniform, so there would be no edge effects due to fringe fields. Thus the "effective volume" of the target gas from which the ions were drawn was the rectangular parallelepiped defined by the active segment of the two collector assemblies. Edge effects at one end of this volume which were due to forward momentum of the slow ions should have been exactly compensated by the same effects at the other end, since the incident fast beam was not attenuated or scattered appreciably across the volume.

In front of the positive ion collector assembly was placed a grid consisting of 0.004-inch diameter stainless steel wires strung 0.100 inch apart on a brass frame, and spaced 1/4-inch in front of the collector plate surface. The grid was held negative with respect to the collector to suppress the emission of secondary electrons. The other plate assembly which was held positive to collect electrons and negative ions did not require a suppressor. The photograph of the collection assembly in Figure 6 was taken while a grid was in front of the electron collector. After this photograph was made this grid was removed and the electron collector plates

were moved in toward the beam axis, so that the negative ion collector plates and the grid on the positive ion collector were symmetrical about the beam axis and 1/2-inch apart. The ion transmission of the grid was assumed to be essentially equal to its geometric transmission, which was 96 per cent.

A fraction of the "slow" ions produced by energetic helium ions might in fact have had substantial energies of up to 100 ev and more, and their initial motion might of course be directed toward the wrong collector plate. A substantial "collection" field across the collision volume was required to assure that essentially all particles would reach the proper collector. The collection field was determined by the potentials of the suppressor grid and the electron collector. These were maintained at potentials of equal magnitude but opposite sign with respect to the grounded chamber so that the beam traveled the zero equipotential. This magnitude will hereafter be designated as V_c (c for "collection"). The positive ion collector plate was positive with respect to its grid by an amount designated as V_s (s for "suppression"). Thus the positive-ion collector was at the negative potential $-(V_c - V_s)$.

A number of difficulties were encountered in choosing suitable values of V_c and V_s. They had to be chosen large enough that the collected currents would show saturation. Verification checks were made by remeasuring the cross sections for incident protons on hydrogen and helium, for comparison with well established older results. The values that were obtained for σ_+, the apparent cross section for the production of slow positive ions, were found to be in good agreement. However, the values for σ_- computed from the collected electron currents were at first found to be

unsatisfactory. Measurements of the cross sections involving incident helium ions were measured subsequent to solution of this problem.

The magnitude of the collected electron current was found to increase gradually as the magnitude of the collection electrostatic field was increased through the range where a plateau was expected. The current did not level off until the potential of the electron collector was made 400 or 500 volts positive, whereas it was expected that a negligible fraction of the slow electrons liberated in ionization collisions would have energies in excess of about 100 ev. In addition, the value of the electron current when this saturation point was reached was larger than the positive ion current, at energies near 1 MeV, by an amount of the order of 15 per cent. For incident protons at these energies, it was well established that the electron current should be equal to the positive ion current. This is expected because the known charge-transfer cross sections for protons are at least two orders of magnitude smaller than the measured ionization cross sections;[18] the expected equality of the currents had been confirmed repeatedly in earlier work.[17]

Further study of this matter led eventually to the suspicion that the excess electrons were fast electrons coming into the chamber from the beam entrance aperture. Presumably they are "knock-on" secondaries produced by the grazing impact of fast beam ions on slit edges. Problems with such electrons had been encountered in the past, but were thought to have been eliminated by careful construction of the beam collimator. It now appears that despite these precautions, such secondaries remain a problem that must be treated with care.

The gradual increase in the collected electron current with increase of the ion collection field is now believed to be due to deflection of a steadily increasing fraction of these fast secondaries to the electron collector. If the collection field were to be made great enough, all these secondaries could be deflected to the guard electrode before they reached the active electron collector.

Alternatively, if the collection field were to be made sufficiently small, most of the fast secondaires would pass completely through the sensitive volume without sufficient deflection to reach the collector. Of course, the field cannot be made too small or there will no longer be efficient collection of the slow ions and electrons produced by true ionization in the target gas.

Accordingly, further tests were made using potentials on the electron collector of less than 100 volts, corresponding to smaller collection fields than we had ever used previously in this experiment.[17] In Figure 7, I^+/I_i and I^-/I_i are plotted versus collection voltage. It was found that the electron current saturates for potentials of about 90 volts, and displays a satisfactory plateau in the region from 80 volts to about 160 volts. The aforementioned rise sets in only for potentials above 160 volts, and continues, as stated above, up to 500 volts. At the same time, the collected positive ion current also saturates at about 50 volts and remains constant. The electron currents obtained for voltages within the plateau were equal to the positive ion currents within 4 per cent for incident protons at energies near 1 MeV. The cross sections obtained for incident protons were now in entirely satisfactory agreement with older results.[17]

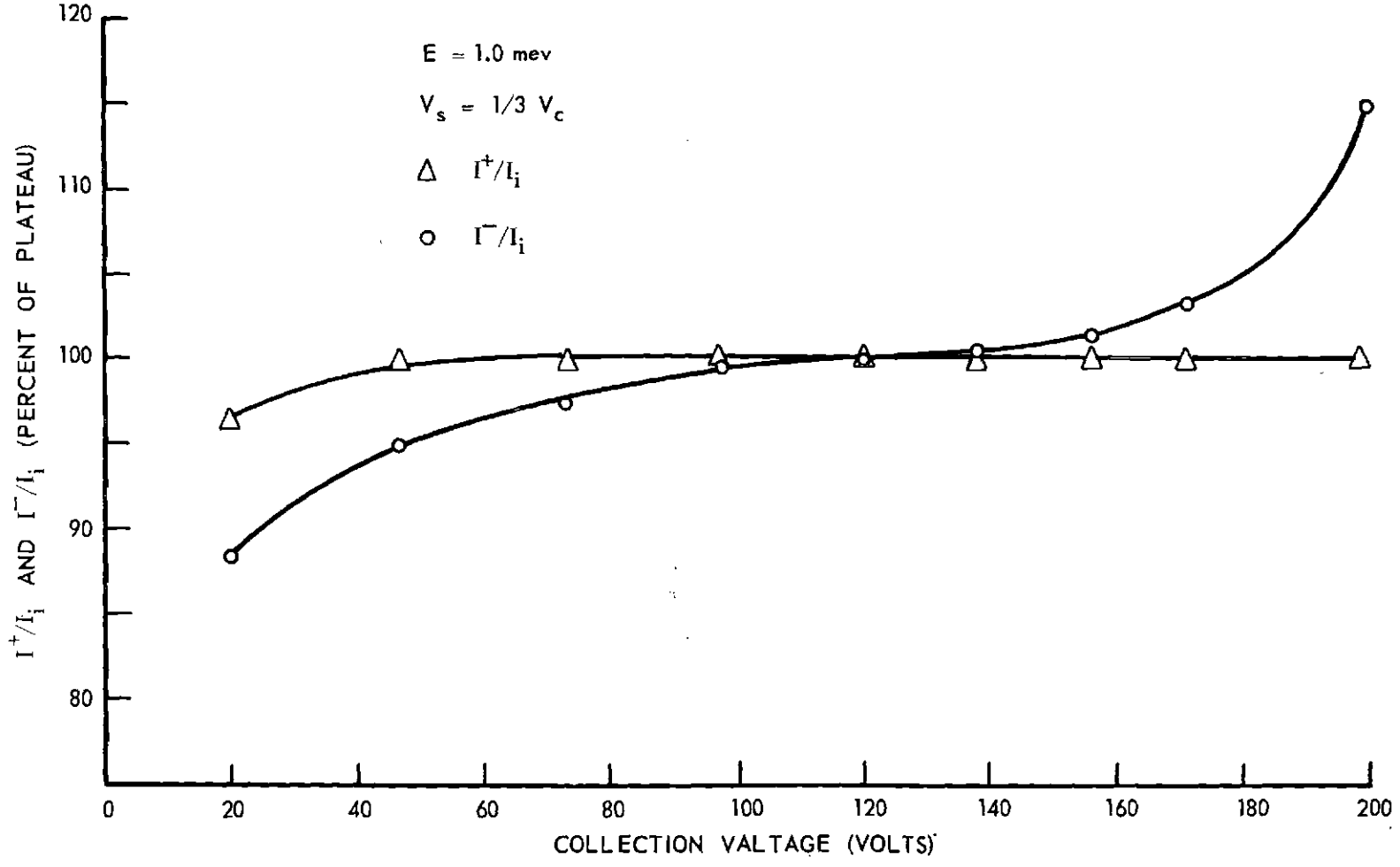

Figure 7. Apparent Ion and Free Electron Currents Versus Collection Voltage for H^+ Incident on H_2.

It is believed that this mode of operation is successful only because the collimation of the incident beam is such that the secondaries entering the collision chamber through the beam entrance aperture are almost entirely limited to a selected high energy group of almost dead-ahead knock-ons. Since the mean energy of this group is related to the energy and mass of the incident ions, the plateau has been carefully checked at several energies covering our range for both incident protons and He^+ ions. A collection voltage of about 120 volts appears to be satisfactory for most cases, but was rechecked at frequent intervals in the experiment.

It should be added that the contamination of the beam with these fast electrons does not seriously perturb the results of the experiment because of ionization of the target gas by the electrons. The number of these electrons is only about 15 per cent of the number of slow electrons liberated in the gas by ionization collisions, but this current in turn is never more than 4 per cent of the incident beam. The beam contamination amounts at most to a fraction of 1 per cent due to both charge-changing collisions and fast electrons. The fast electrons presumably have speeds of the order of twice the speed of the ions, so in our energy range the ionization cross section of the electrons will always be less than that of the ions.

The two Keithley model 410 electrometers used for current measurements had to be floated from laboratory ground at the potentials of the collectors. They were isolated from their mounting rack by lucite blocks and were completely enclosed by a well-grounded screen cage. AC power was supplied through isolation transformers. The DC polarizing potentials were supplied by shielded battery packs which were also enclosed in the cage,

because any ripple or noise in this supply was capacitively coupled into the electrometer input. Under these conditions, the noise in the electrometers with no input current was such as would have interfered with current measurements in the 10^{-13} ampere range, but it was negligible for the smallest currents (2×10^{-12} amperes) encountered in the measurements described. A Keithley model 415 electrometer was used to measure I_i. The case of this electrometer was grounded.

The most serious source of noise in these experiments came directly from the behavior of the incident ion beam. Although the current entering the collision chamber had satisfactory long-term stability, its instantaneous value varied rapidly and erratically. Damping time constants provided by shunting capacitors in the meter circuits of the electrometers were added to reduce the meter jitter. The meters were in close physical proximity so that all could be seen at the same time. The ratios I^+/I_i and I^-/I_i could be observed to an estimated 4 per cent maximum uncertainty, including both reading error and the inherent uncertainty of the electrometers. The roles of the two Keithley model 410 electrometers were interchanged periodically to ascertain if any systematic error had developed. These electrometers were returned to the factory midway in the experiment for recalibration.

A most important factor that has not yet been mentioned is that of leakage currents. The construction of the collector assemblies was such that the leakage paths from the active collector segments across the teflon mounting plate to the grounded collision chamber were long and of very high resistance, and the resulting leakage currents across the teflon were negligible. The leads to the kovar-glass seals in the chamber wall were stiff

copper wires that did not touch any surface. Each of the leads from the outside end of a seal to the electrometer cage was doubly shielded by the use of a coaxial cable with a heavy rubber outer jacket, slipped inside an extra braided wire sleeve. Only the outermost shields were grounded, while the inner shields of all cables were held at the same potentials as their central current leads. The kovar-glass seals themselves were, however, unguarded since they were not of a double concentric type that would permit the same arrangement as in the cables.

Leakage currents, while not strictly ohmic, were small and steady and varied with collection voltage in a regular way. They reproduced well over periods of hours, although there was some day-to-day variation that was presumably related to atmospheric conditions. The leakage current was read at frequent intervals during all data runs.

The arrangement of the high-voltage connections seen in Figure 8 may be summarized as follows:

The central segment of each collector assembly had a separate lead. The remaining four outer guard segments were connected electrically. The grid of the positive ion collector had a separate lead. All leads passed out of the vacuum through separate kovar-glass seals, and through separate doubly shielded cables to a lucite patch board inside the electrometer cage.

The high-voltage tap of the polarizing battery pack was connected to a 5 megohm potentiometer. The center tap was connected directly to the electrometer frame and to the inner shields of the two leads from the guard and active segments of the collector. The physical arrangement was such as to avoid any "loops" for pickup. The leads from the outer guard

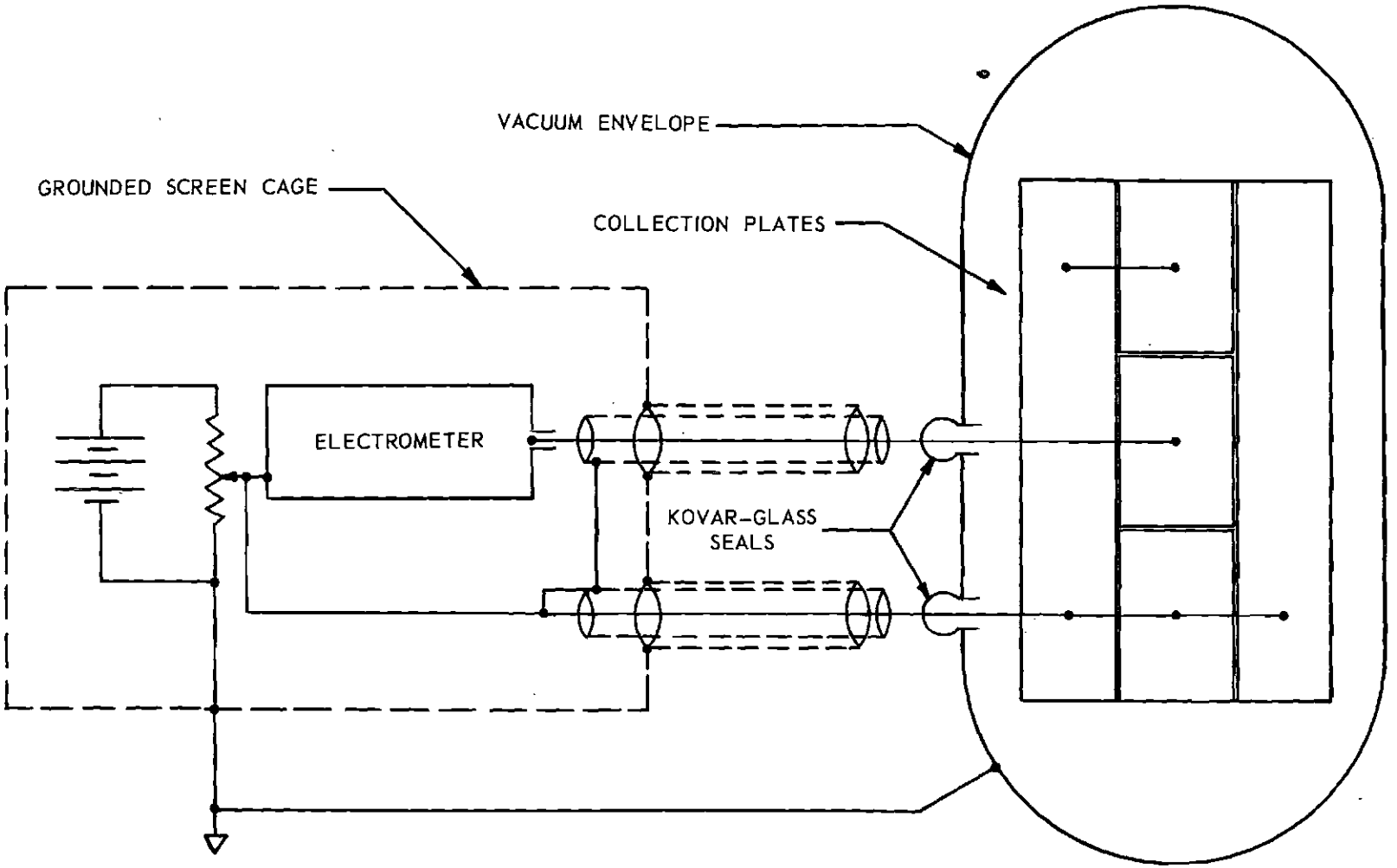

Figure 8. Schematic of Electrical Connections.

segments were also connected directly to the center tap of the 5 megohm potentiometer.

The internal feedback arrangement of the electrometer limited the potential difference between the input and the frame to a few millivolts for any value of the input current, so that the active segment had essentially the same potential as the guards.

CHAPTER V

EXPERIMENTAL RESULTS

Summary of Experimental Method

The cross sections for the production of slow positive ions and free electrons for He^+ ions incident on helium, neon, argon, hydrogen, nitrogen, oxygen, and carbon monoxide were measured for incident particle energies over the range from 0.133 to 1.00 MeV and similar cross sections were measured for He^{++} ions incident on helium and hydrogen for incident particle energies over the range from 0.50 to 1.00 MeV. The incident ion energy was determined by 90° deflection in a regulated magnetic field, whose value was measured with a precision gaussmeter. The slow ion and electron currents were measured simultaneously with the incident beam current by means of sensitive electrometers. The target gas pressure was measured by a liquid-nitrogen-trapped McLeod gauge and ranged from 0.50×10^{-4} Torr to an upper limit of 10.0×10^{-4} Torr for gases with small cross sections. The effective collision volume was determined by the use of guard structures around the collector electrodes. Collection potentials of plus and minus 90 to 160 volts were used for the bulk of the measurements. A suppression potential of 30 to 50 volts was used between the positive ion collector and its associated grid.

Data Corrections

Leakage currents in the electrometer circuits were measured frequently and subtracted from all current measurements for which they had a

significant value. The correction was usually less than 1 per cent. The constant pumping arrangement described in Chapter III was used to provide a residual background gas density that was independent of the sample gas density insofar as possible. The target gases were admitted through a mechanical leak subsequent to liquid nitrogen or dry ice and acetone trapping.

The actual pressure of the background gas could not be determined because of uncertainty as to its composition. The pressure indicated by an ionization gauge, using the calibration for nitrogen, ranged up to 3×10^{-6} Torr. However the pressure indicated by the McLeod gauge was always less than 5×10^{-7} Torr. It was concluded that the bulk of the background consisted of condensible vapors from gaskets, pumps, etc., rather than of leaking air or permanent gases outgassed from surfaces. Such condensible gases would be expected to have large ionization cross sections and thus contribute to the total ionization out of all proportion to their actual density. Therefore the ionization currents produced in the residual gas were measured frequently and subtracted from the currents obtained with target gas present, constituting corrections up to but never more than 10 per cent. However it was assumed that the reading of the McLeod gauge corresponded only to the partial pressure of the target gas, and its readings were therefore not corrected for background.

Because this procedure depends on the assumption that the background gas density is the same when the target gas is present as when it is not, it is only approximately correct. It was found that data taken at very low target gas pressures, for which the background correction was much greater than 10 per cent, failed to agree with data taken at higher

pressures. Therefore data used in the compilation was taken only with pressures great enough that the background correction was less than 10 per cent.

A set of values obtained for the cross section σ_+ at one energy from a series of runs at different pressures of hydrogen gas is shown in Figure 9 plotted to a relative scale. The apparent falloff at pressures below 1.0×10^{-4} Torr exemplifies the situation described for which the background correction became too large. Similarly, the indication of rising values for pressures above 10×10^{-4} Torr was identified with multiple collisions and failure of the "thin target" assumptions. The existence of a definite plateau between these regions lent confidence that all the important assumptions were valid there. All of the data used in compiling the final results were taken from runs lying within this plateau. In computing the molecular density of the target gas, its temperature was taken to be that of the room.

Results

The experimental results of other investigators which are available are included with present results for the cross sections σ_+ and σ_- which are presented for the projectile He^{++} on helium and hydrogen in Figures 10 and 11, and for the projectile He^{+} on helium, neon, argon, hydrogen, nitrogen, oxygen, and carbon monoxide in Figures 12 through 18.

Cross-correlations between total production cross sections and charge-changing cross sections are presented in Figures 19 through 24. For the projectile He^{++}, $\sigma_+ - \sigma_-$ should be equal to $\sigma_{21} + \sigma_{20}$, and for the projectile He^{+}, $\sigma_+ - \sigma_-$ should be equal to $\sigma_{10} - \sigma_{12}$, as was explained

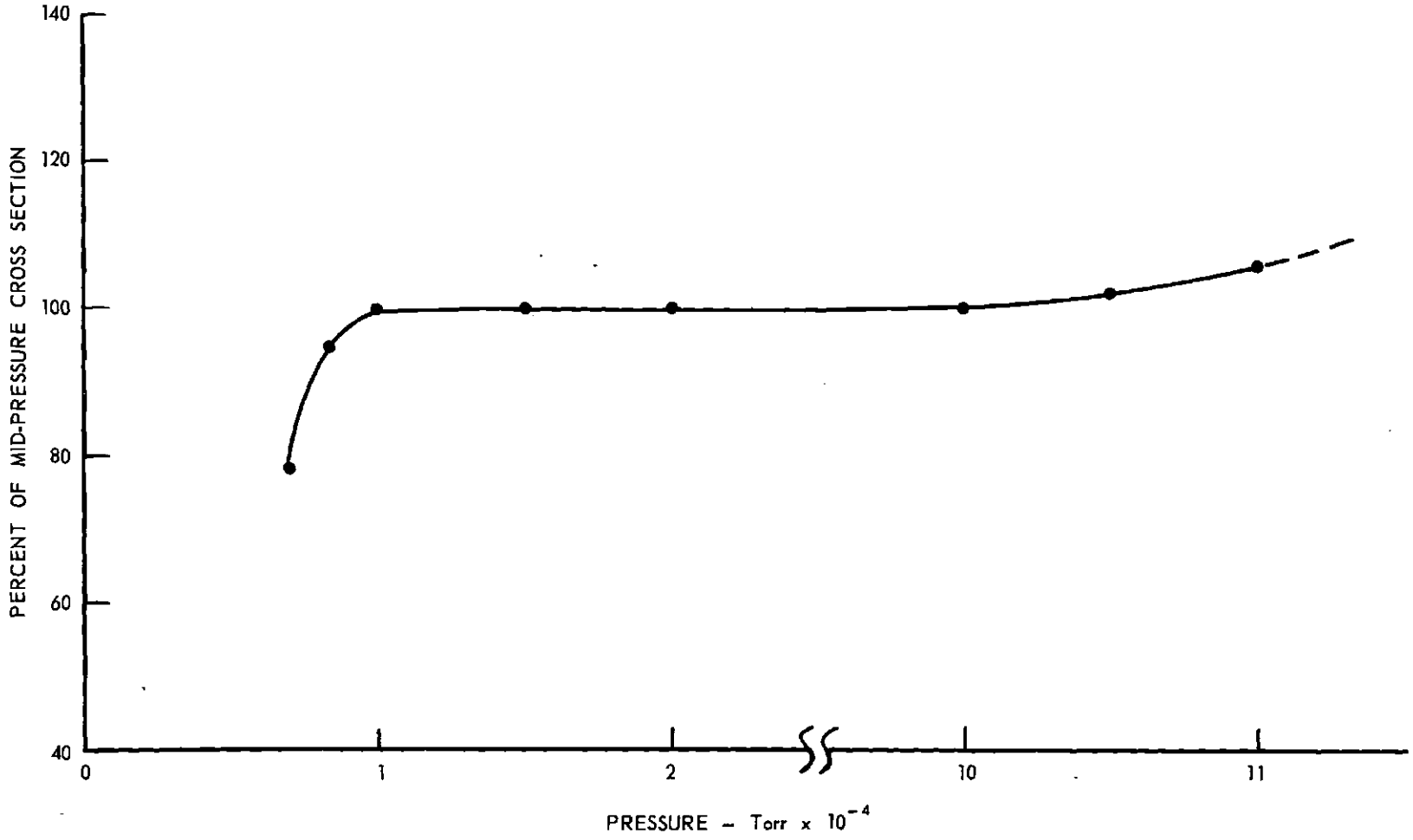

Figure 9. Computed $\sigma+$ (1 MeV) for Varying Target Gas Pressure for He^{+} Ions Incident on Helium Using a CEC Gm-100 McLeod Gauge.

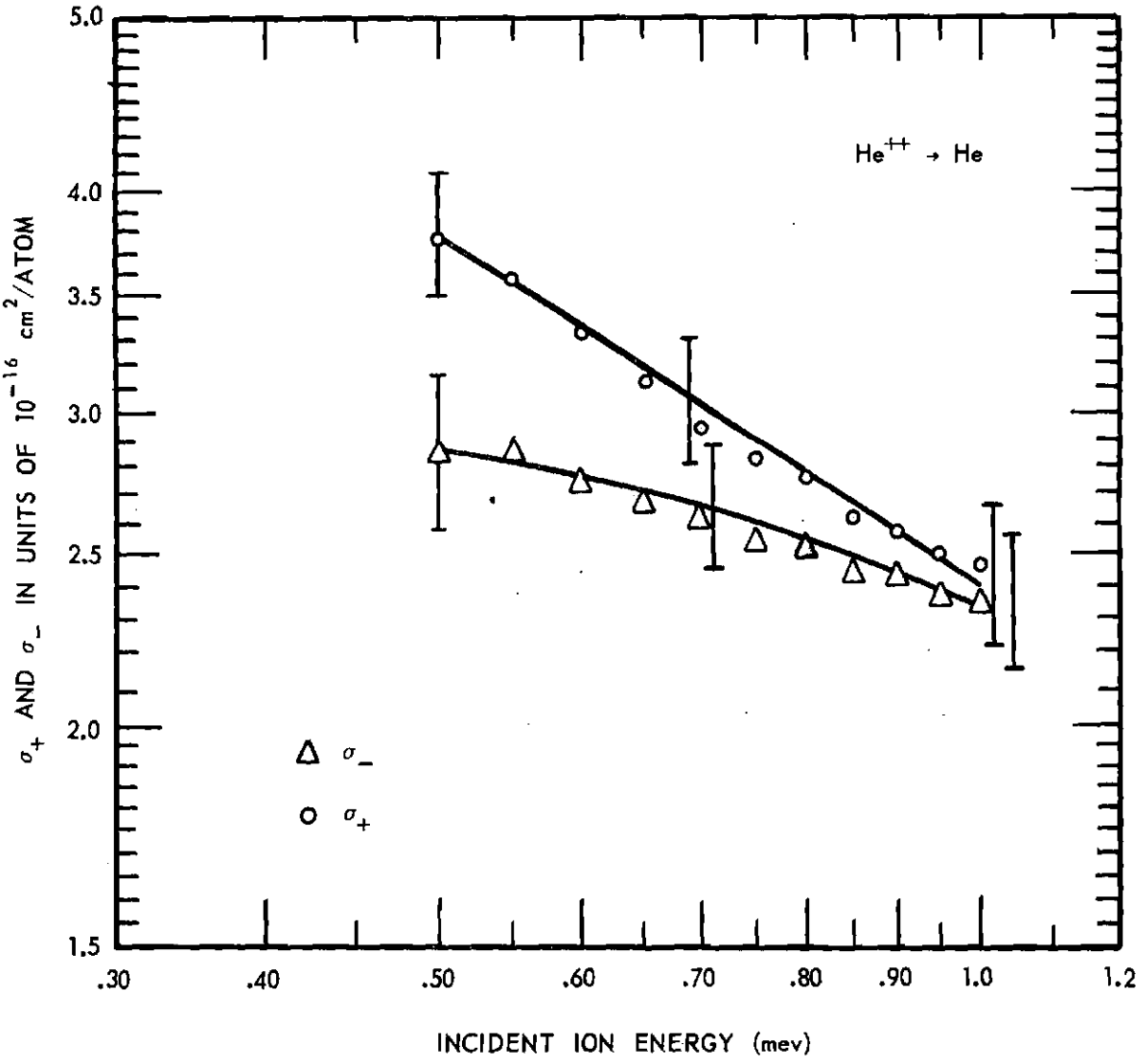

Figure 10. Cross Sections for the Gross Production of Positive Ions and Free Electrons by He^{++} Ions Incident on Helium.

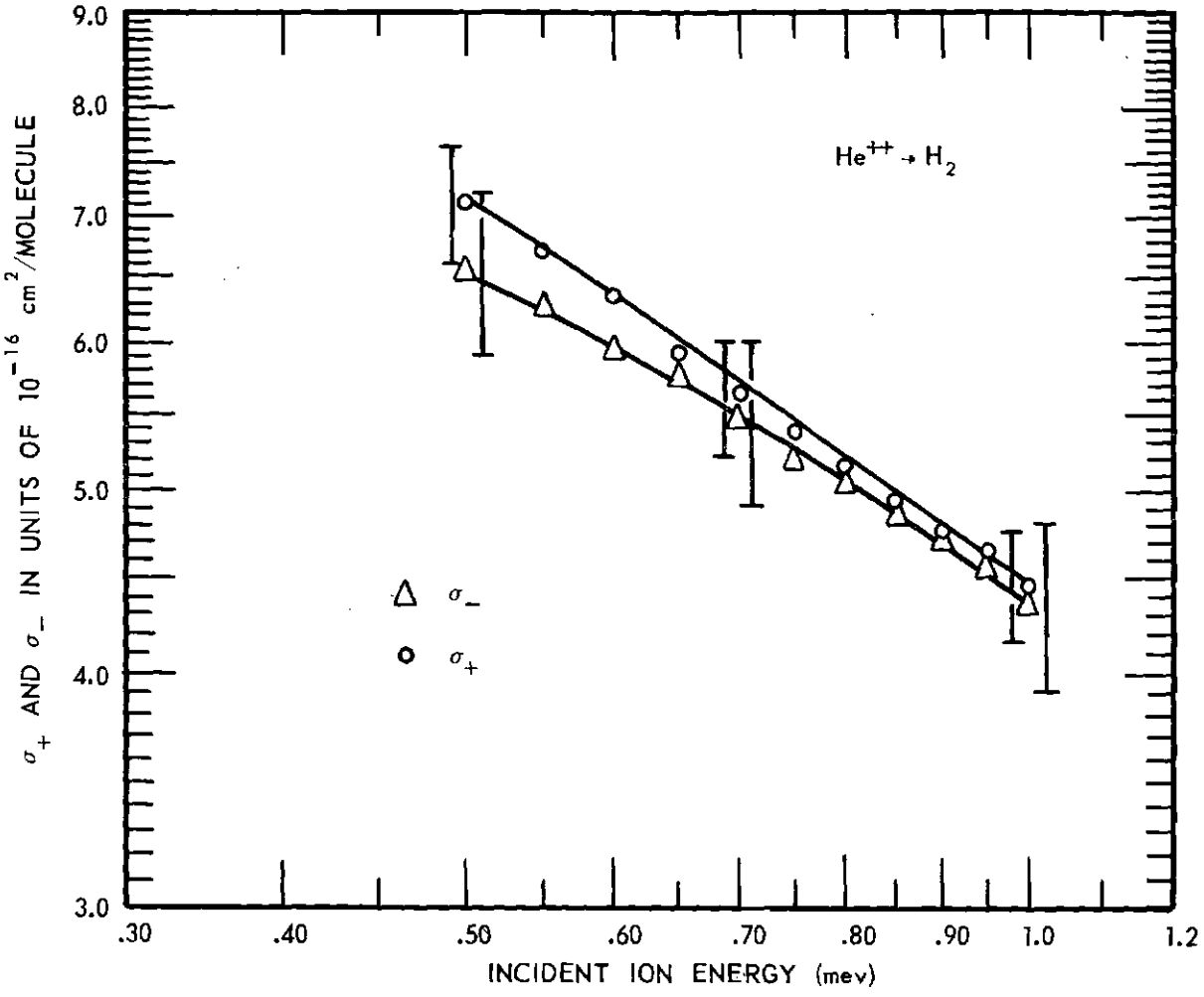

Figure 11. Cross Sections for the Gross Production of Positive Ions and Free Electrons by He^{++} Ions Incident on Molecular Hydrogen.

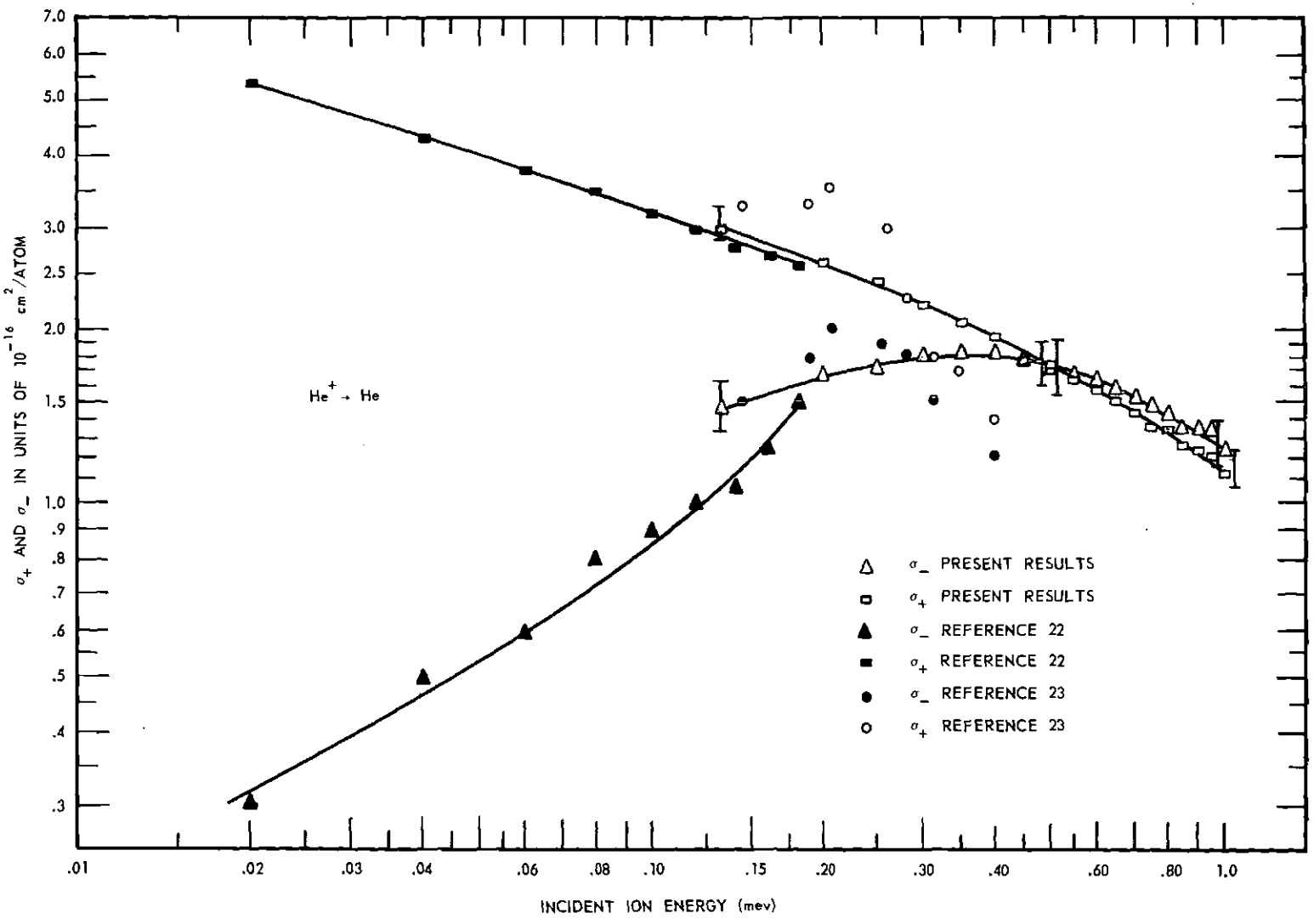

Figure 12. Cross Sections for the Gross Production of Positive Ions and Free Electrons by He^+ Ions Incident on Helium.

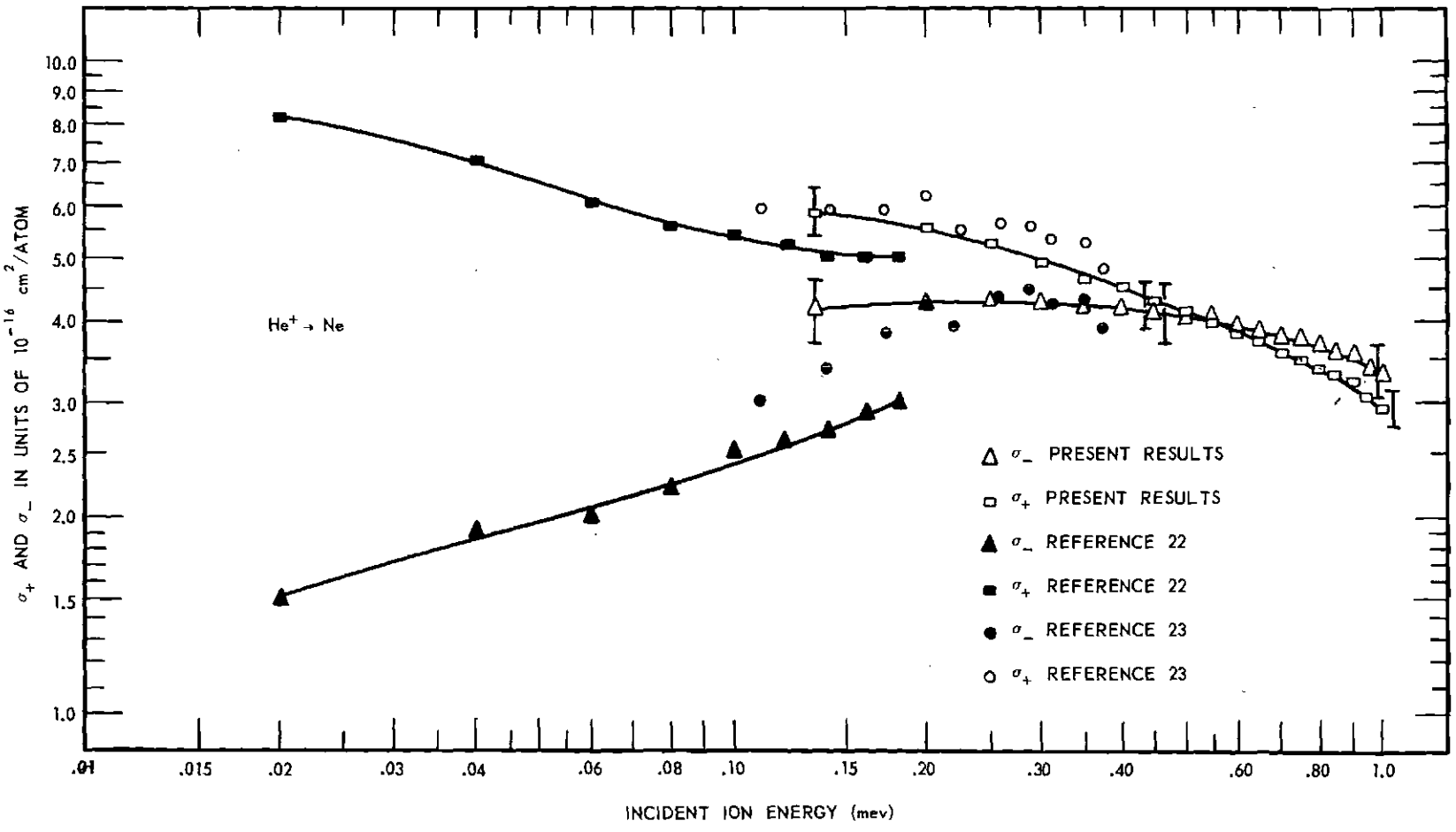

Figure 13. Cross Sections for the Gross Production of Positive Ions and Free Electrons by He^+ Ions Incident on Neon.

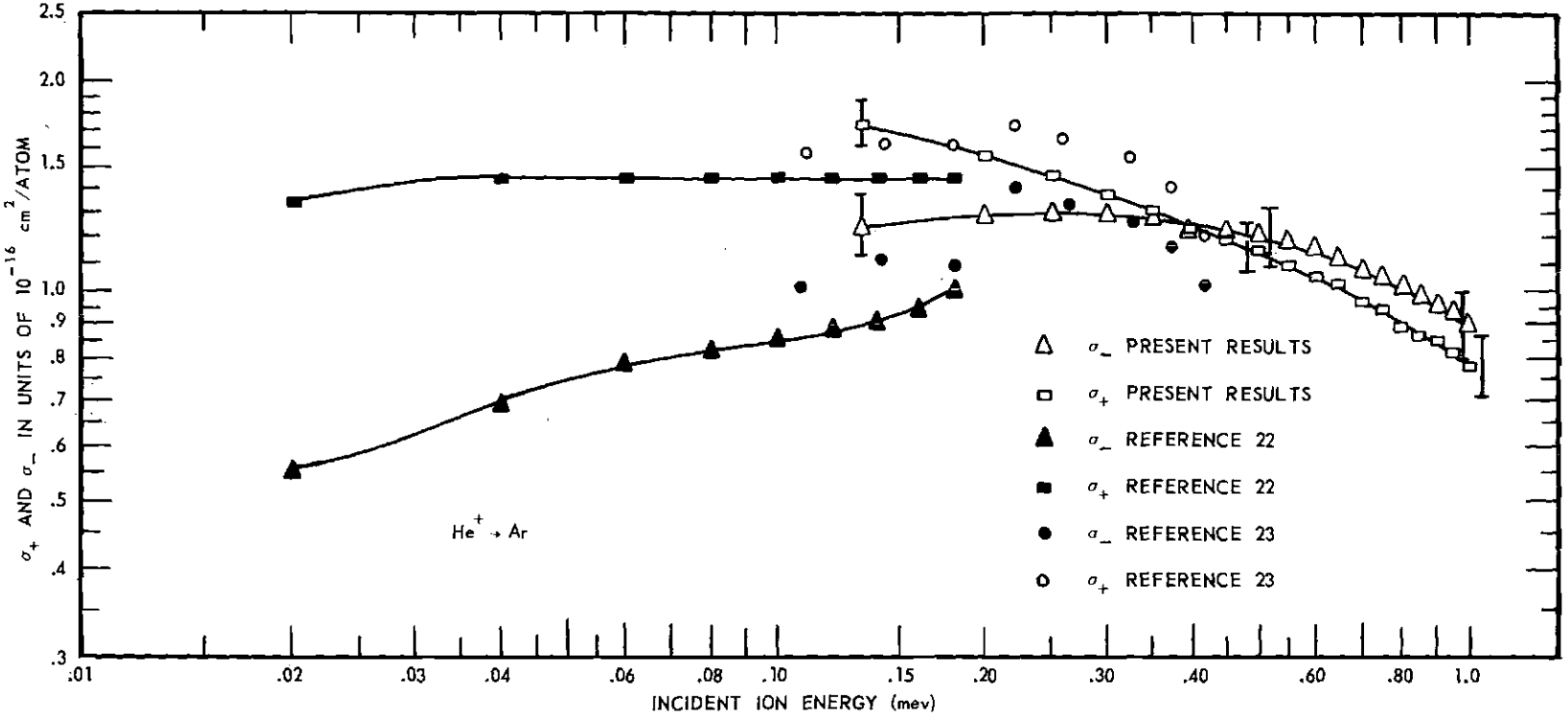

Figure 14. Cross Sections for the Gross Production of Positive Ions and Free Electrons by He^+ Ions Incident on Argon.

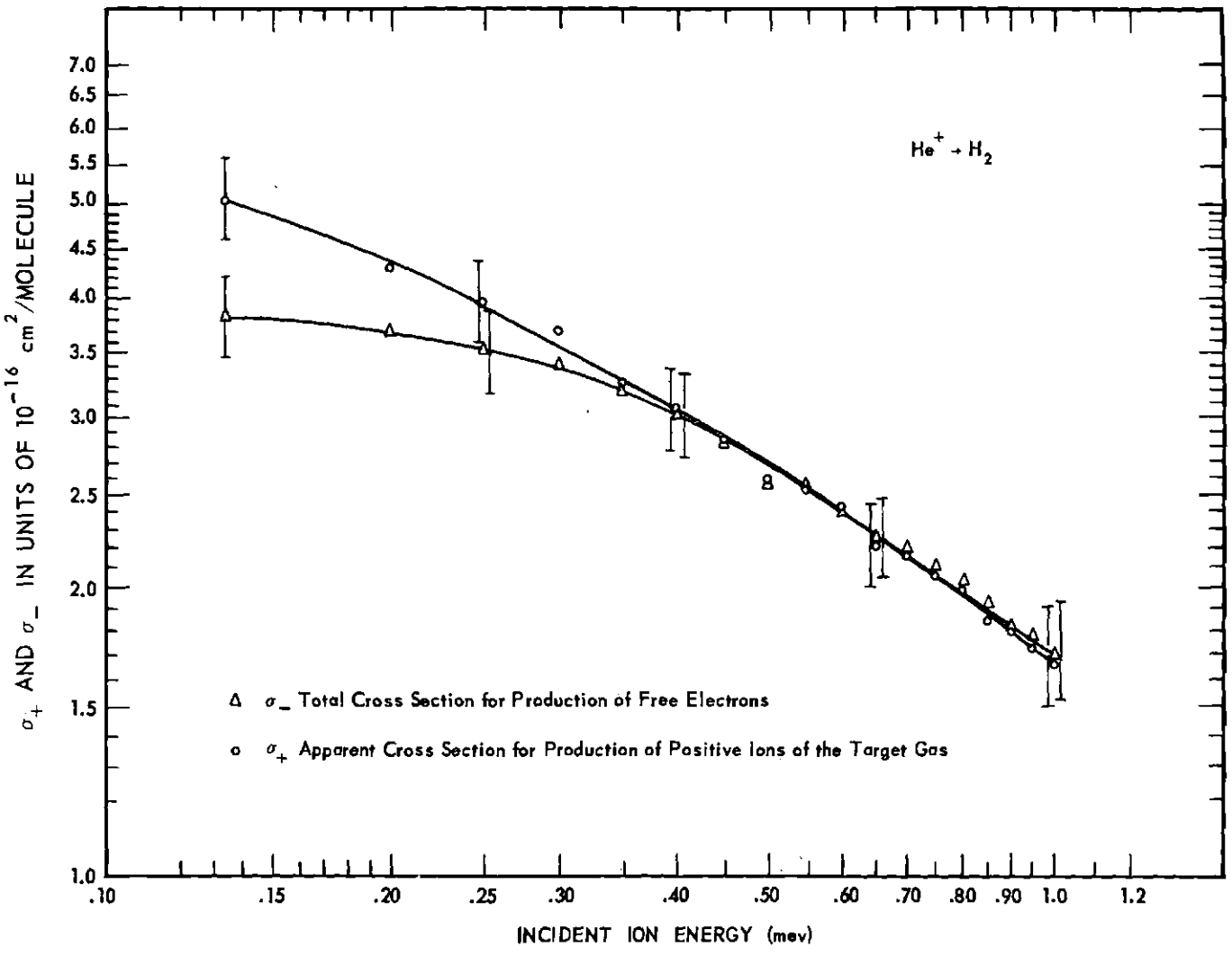

Figure 15. Cross Sections for the Gross Production of Positive Ions and Free Electrons by He^+ Ions Incident on Molecular Hydrogen.

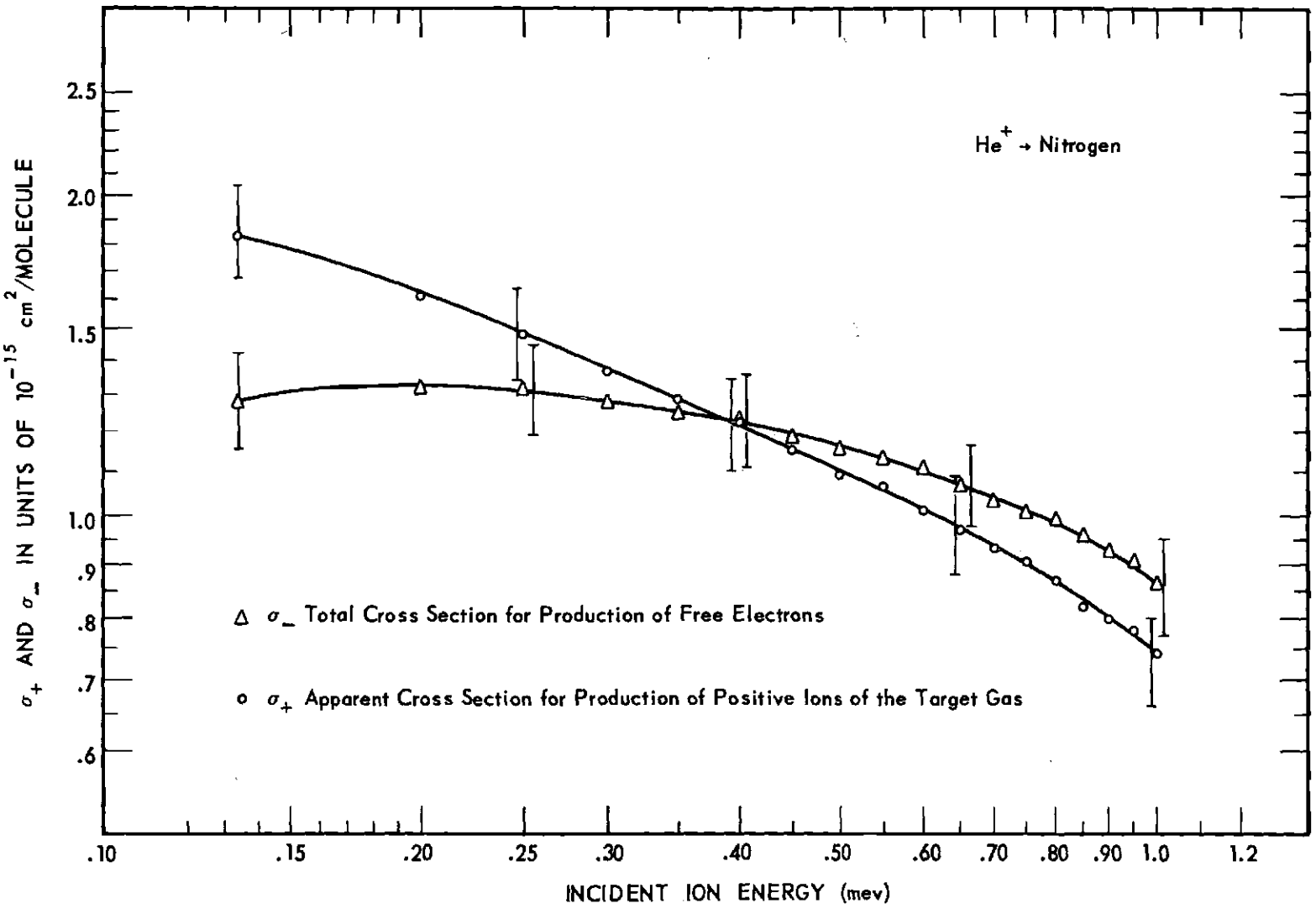

Figure 16. Cross Sections for the Gross Production of Positive Ions and Free Electrons by He^+ Ions Incident on Molecular Nitrogen.

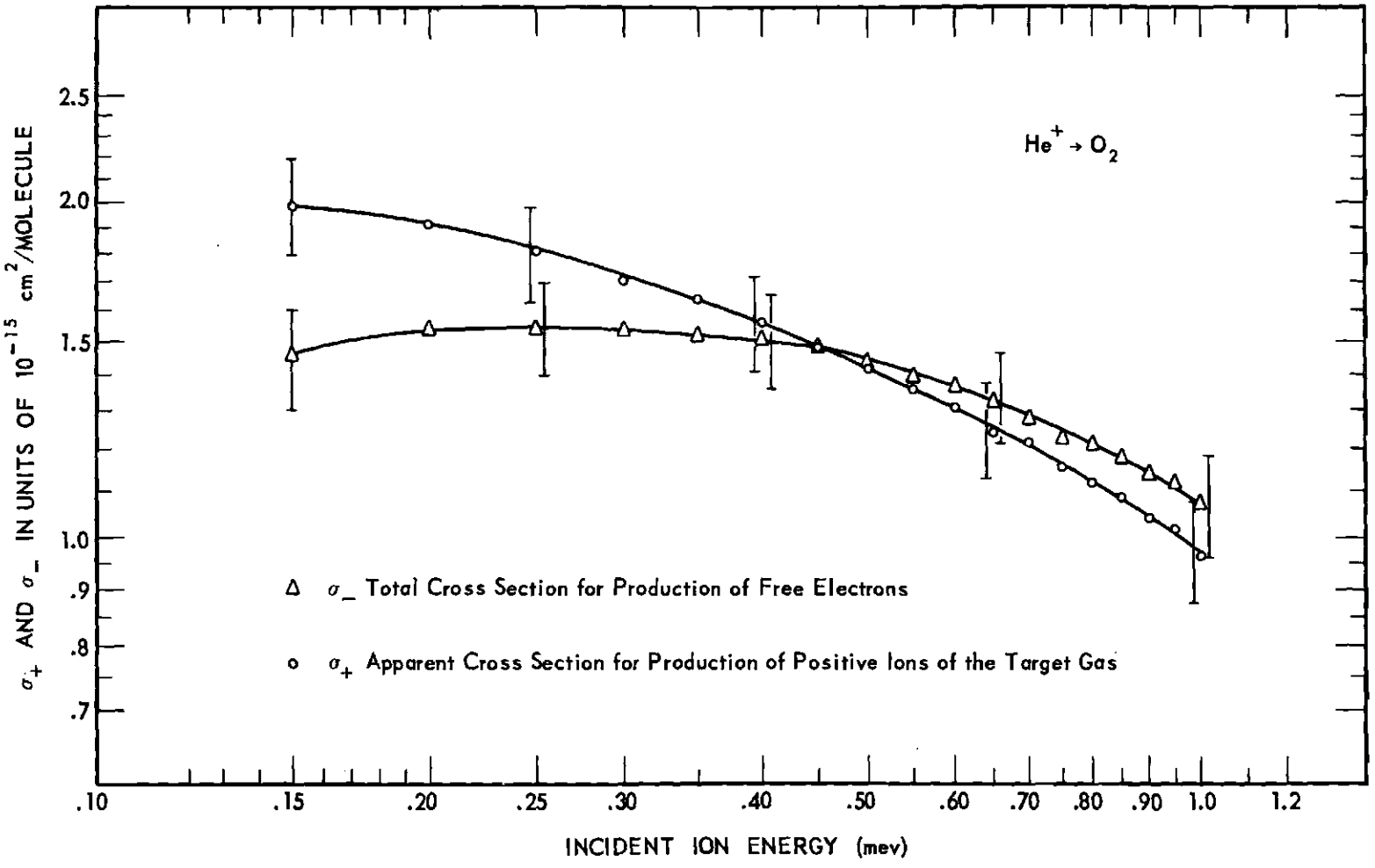

Figure 17. Cross Sections for the Gross Production of Positive Ions and Free Electrons by He^+ Ions Incident on Molecular Oxygen.

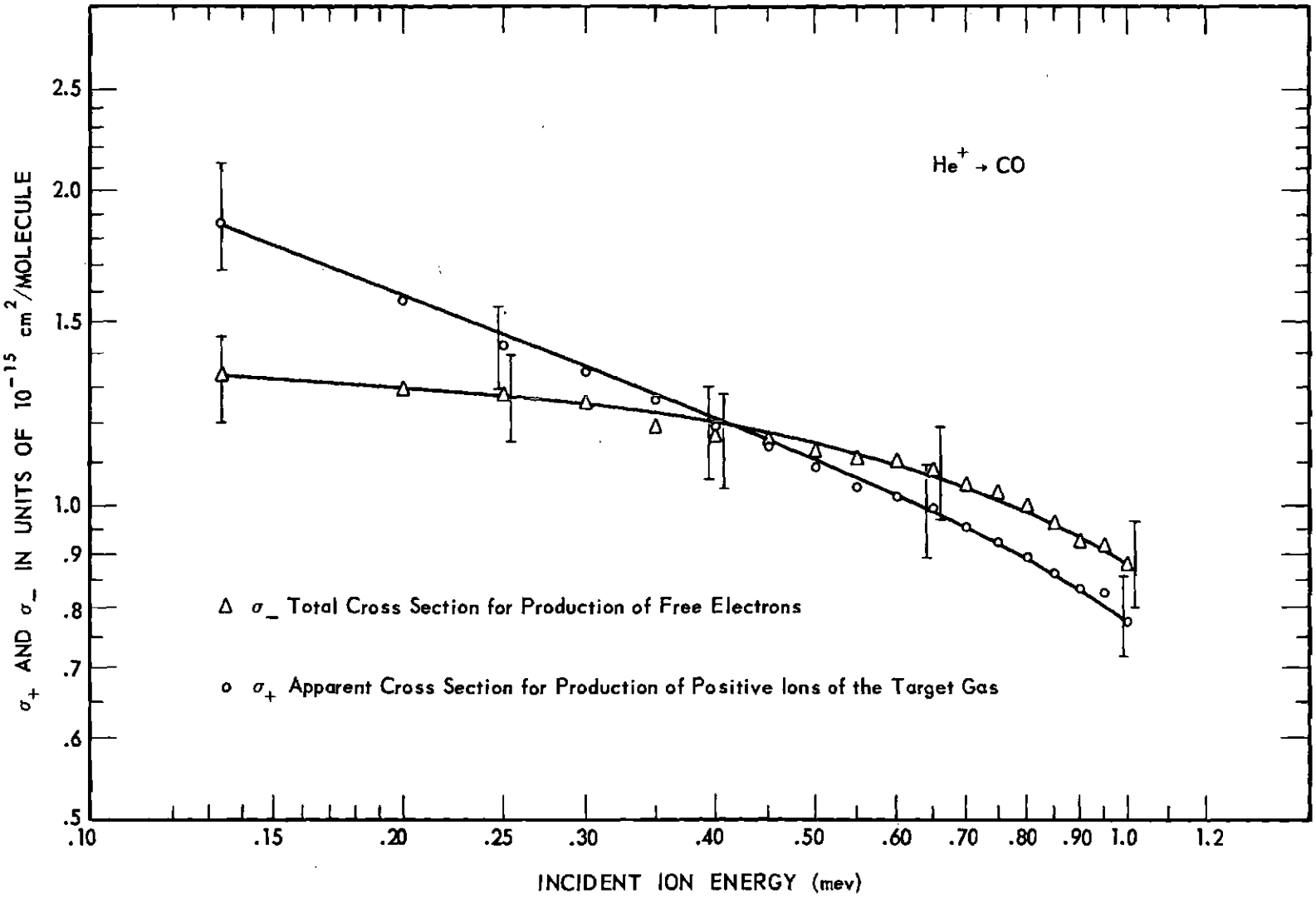

Figure 18. Cross Sections for the Gross Production of Positive Ions and Free Electrons by He^+ Ions Incident on Carbon Monoxide.

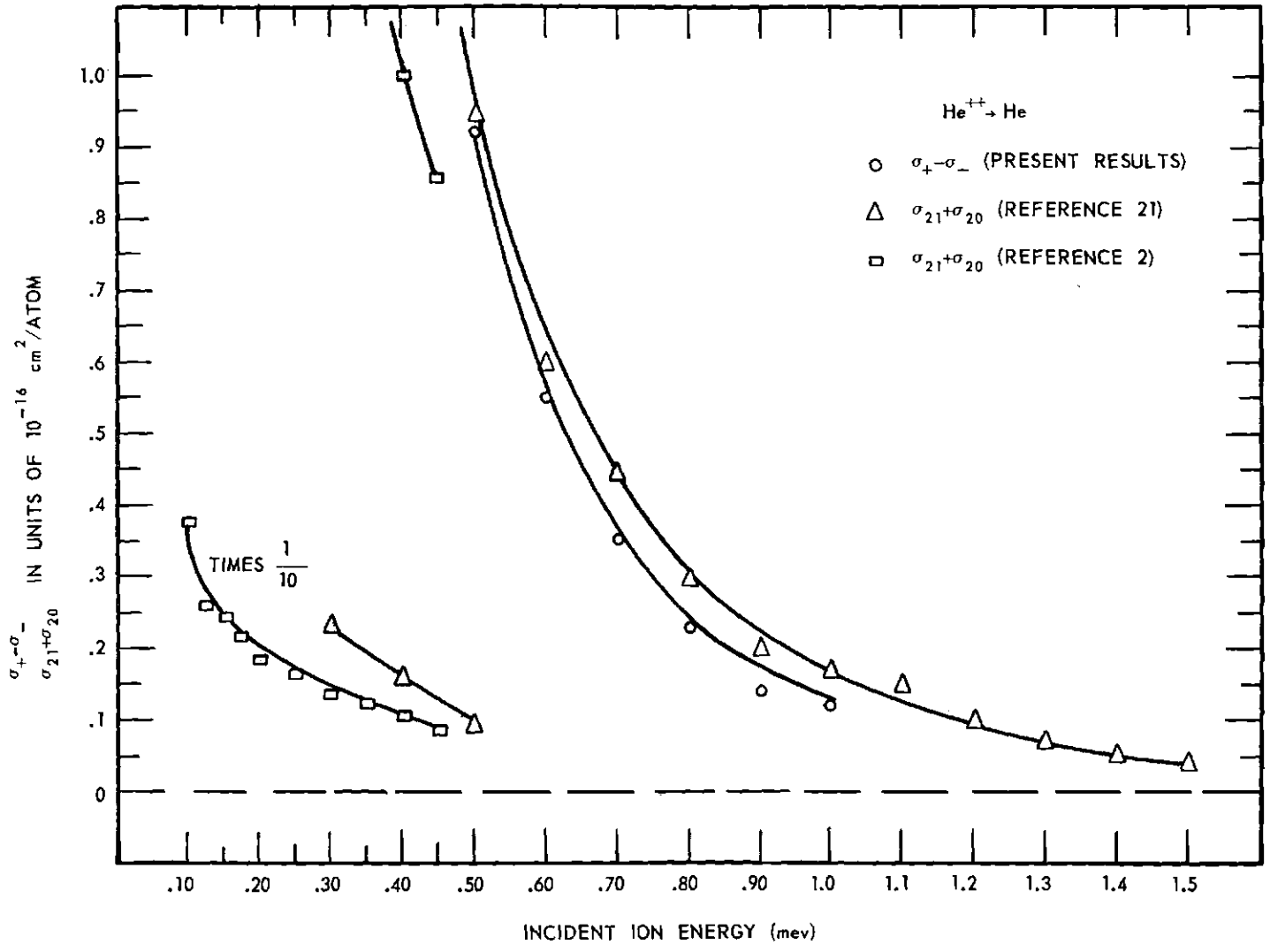

Figure 19. Cross-Correlation Between Total H_e^{++} Production Cross Sections and Charge-Changing Cross Sections for He^{++} Ions Incident on Helium.

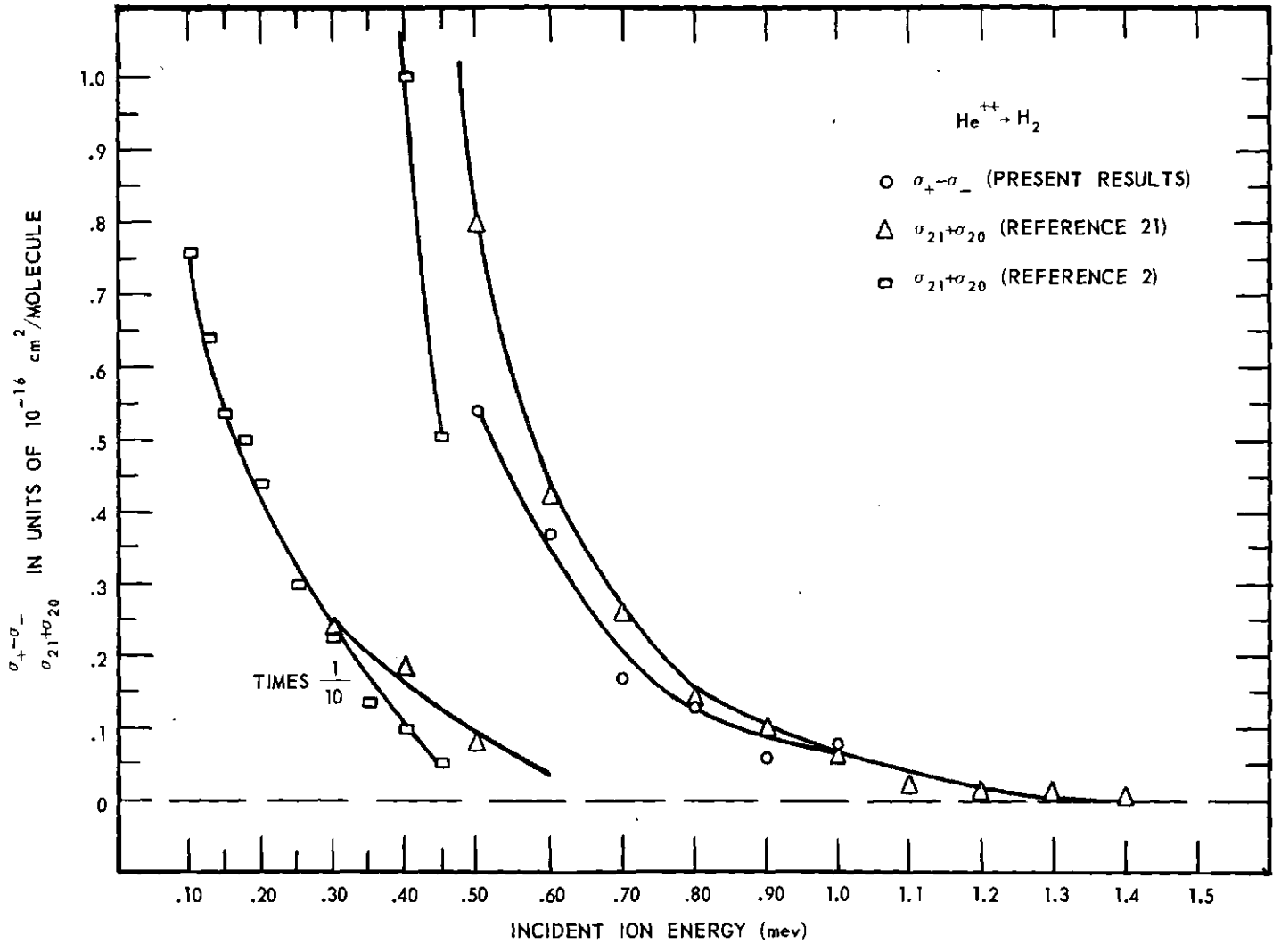

Figure 20. Cross-Correlation Between Total Production Cross Sections and Charge-Changing Cross Sections for He^{++} Ions Incident on Molecular Hydrogen.

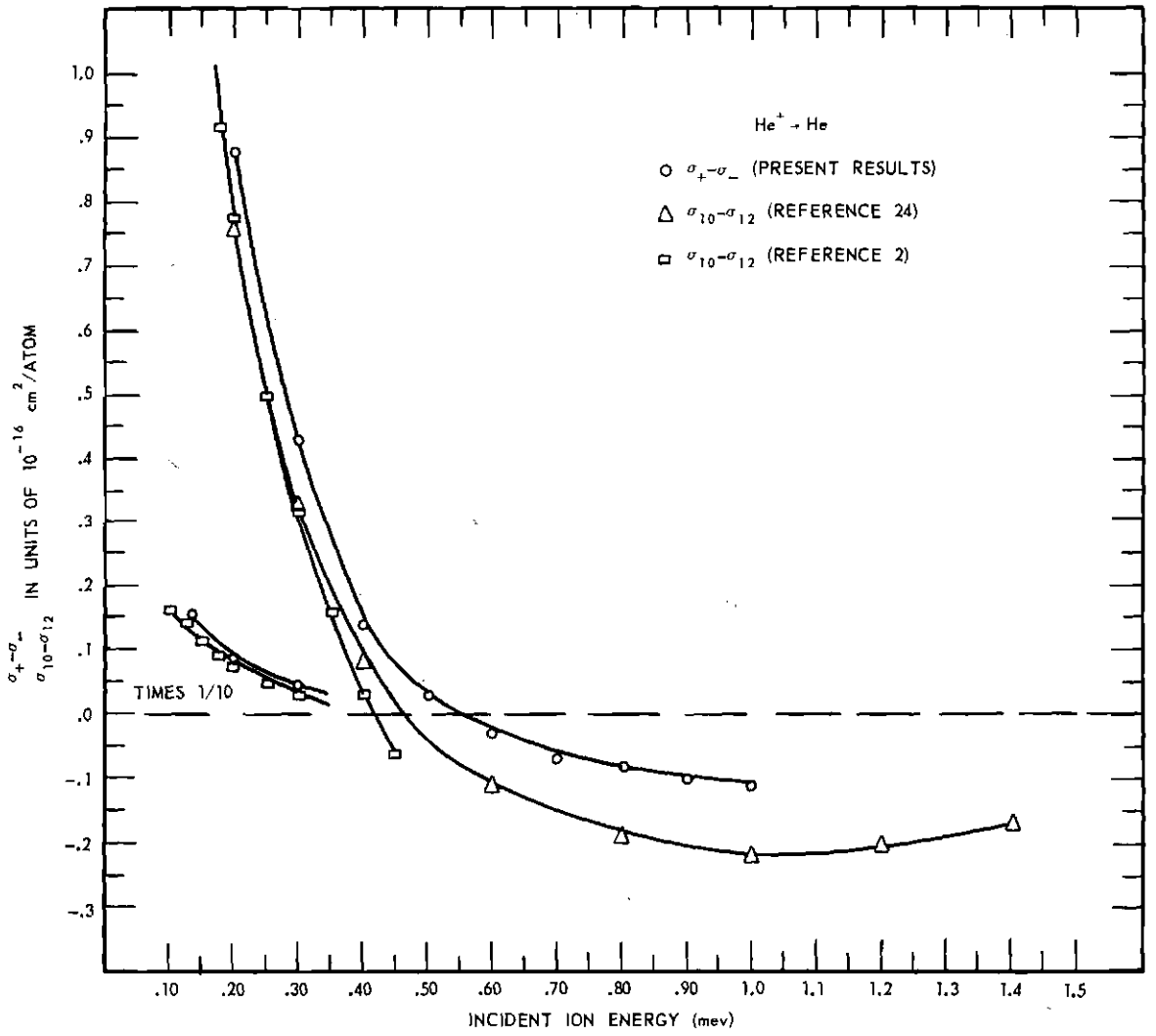

Figure 21. Cross-Correlation Between Total Production Cross Sections and Charge-Changing Cross Sections for He^+ Ions Incident on Helium.

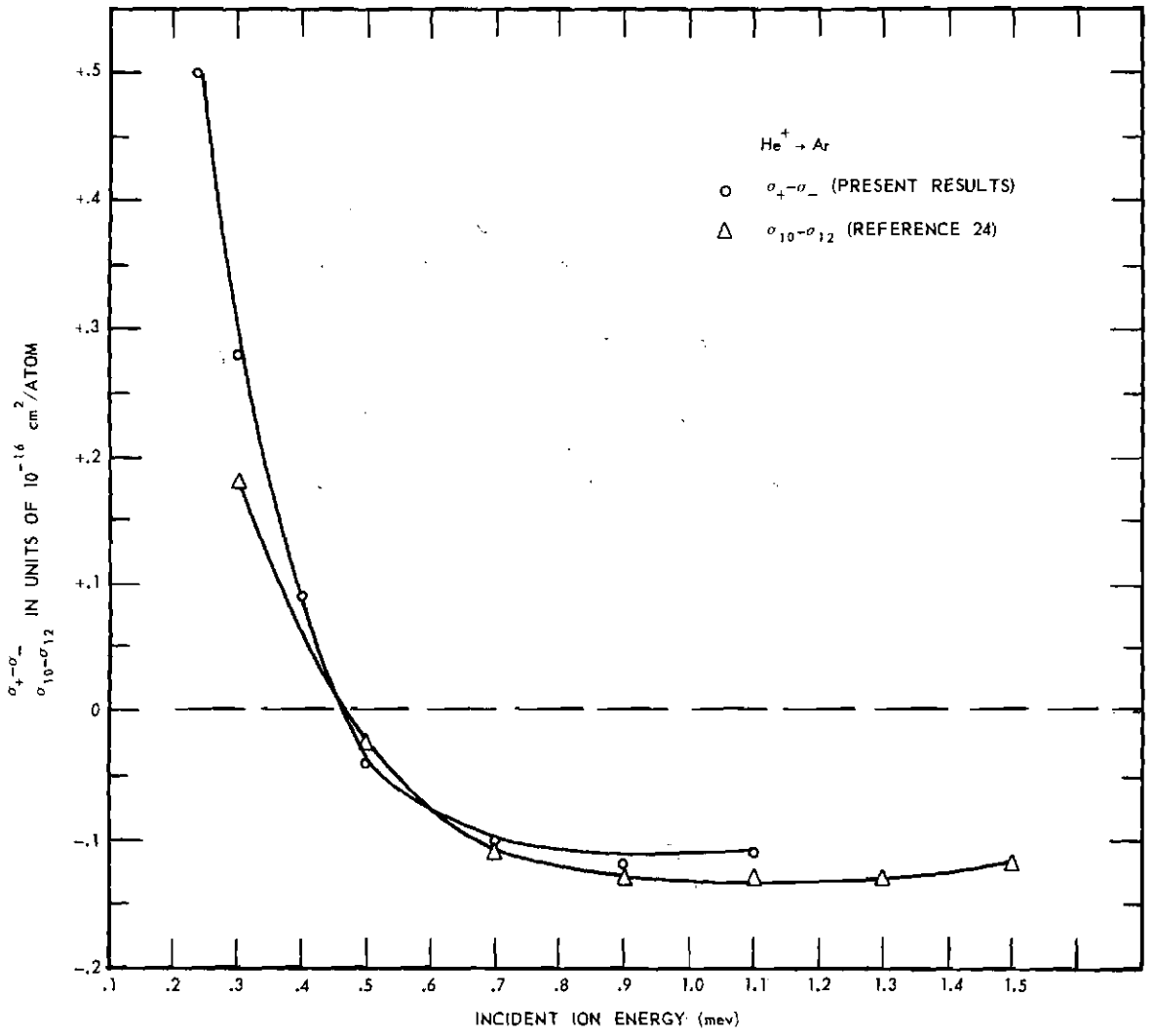

Figure 22. Cross-Correlation Between Total Production Cross Sections and Charge-Changing Cross Sections for He^+ Ions Incident on Argon.

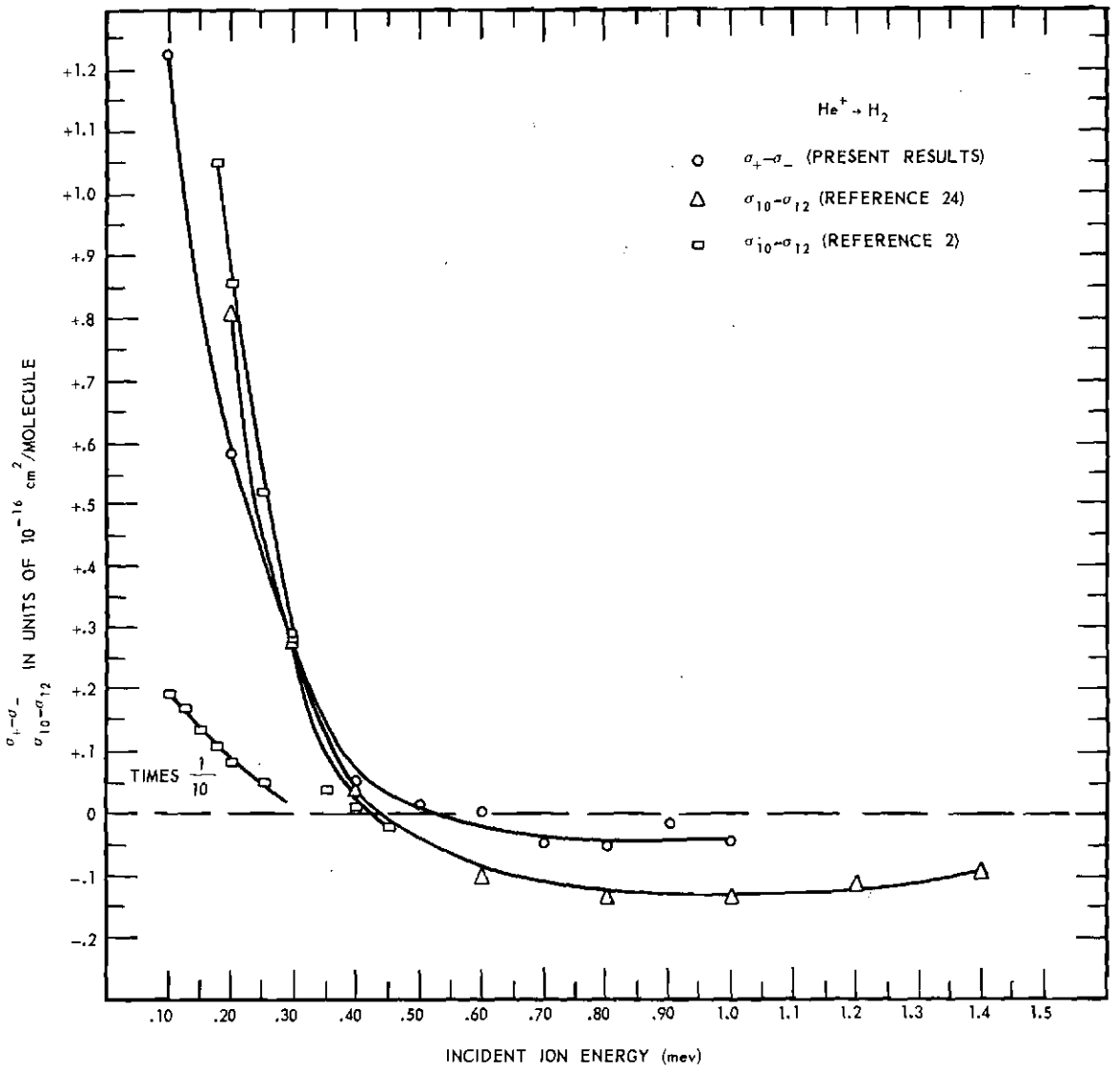

Figure 23. Cross-Correlation Between Total Production Cross Sections and Charge-Changing Cross Sections for He^+ Ions Incident on Molecular Hydrogen.

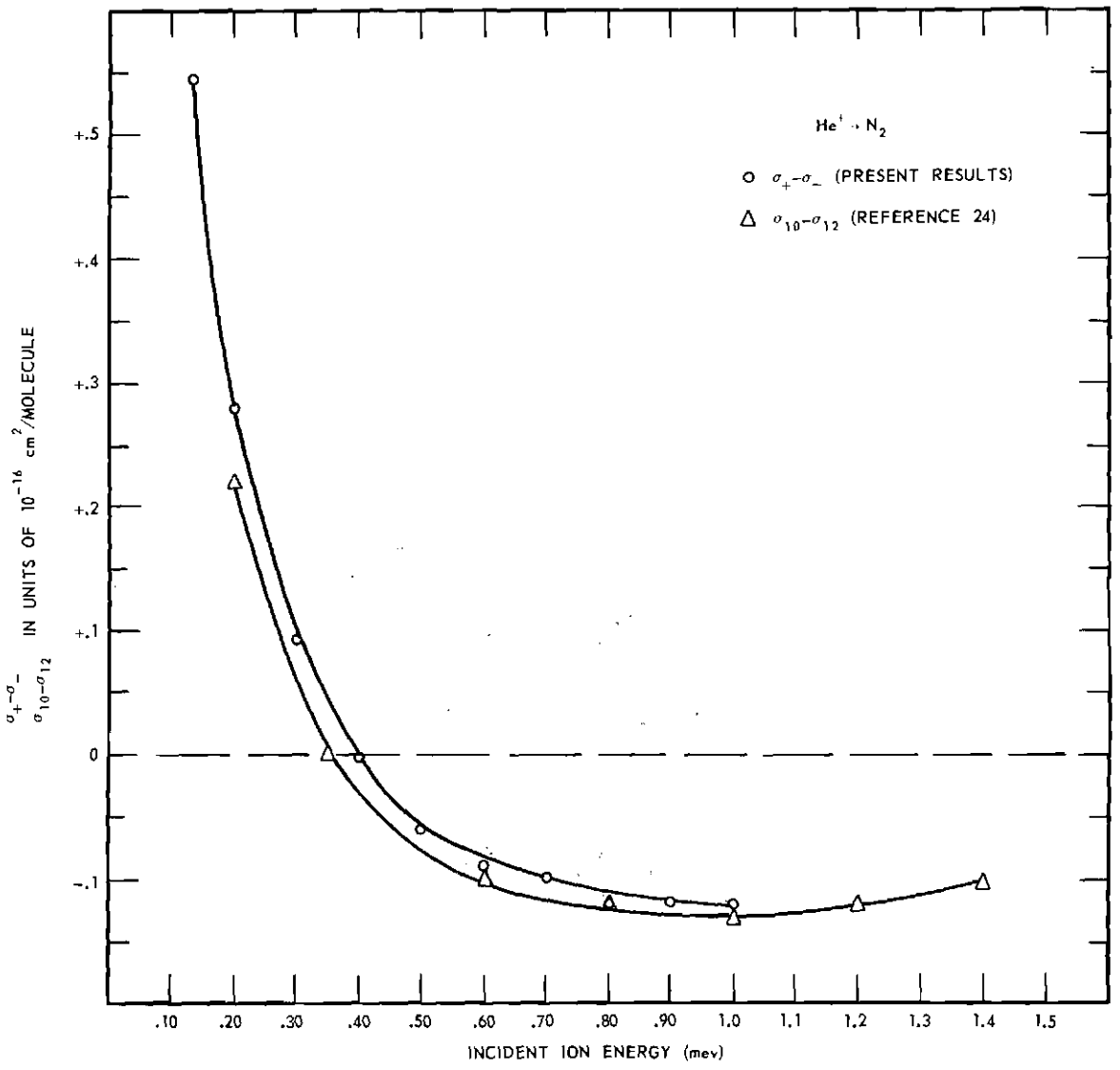

Figure 24. Cross-Correlation Between Total Production Cross Sections and Charge-Changing Cross Sections for He^+ Ions Incident on Molecular Nitrogen.

in Chapter III. The difference between σ_+ and σ_- was always only a fraction of either σ_+ or σ_-; therefore the different sets of data agree well in experimental error and vindicates the method of choosing V_c (see The Collector Assemblies and Electrometers, Chapter IV). Discussion of the possible error brackets shown on the curves is contained in the next section.

Discussion of Errors

It was indicated in Chapter IV that the uncertainty in a single reading of the ratio of the uncorrected ionization current to the incident beam current should not have exceeded about ± 4 per cent. The target gas temperature was not directly measured and may have been uncertain by perhaps ± 1 per cent. By far the largest uncertainty in these experiments lay in the measurement of the target gas pressure. Use of the cathetometer was believed to permit a relative reading uncertainty of the CEC GM-100 McLeod Gauge, used during the He^+ measurements of less than 4 per cent in the range around 1×10^{-4} Torr. This gauge had not been absolutely calibrated, however, so that a possible error of about ± 5 per cent must be admitted in the absolute reading. This led to proportionate possible systematic error in all of the measurements, but it is emphasized that the relative values of the cross sections at various energies are not subject to this systematic error. The CEC GM-110 McLeod Gauge, used during the He^{++} measurements, was calibrated to an accuracy of about ± 1 per cent while deviation of any one pressure reading from an average of about five readings was as high as ± 5 per cent. This error was due to sticking of the mercury column in the capillary and was believed to be random.

As presented in Chapter IV, the excess of electrons found at high collection voltages presented some uncertainty. A plot of I^-/I_i and I^+/I_i on a relative scale versus collection voltage is presented in Figure 7. A discussion of the plot is made there. A lack of knowledge of just what to make the collection voltage led to an additional uncertainty in σ_- of not more than 3 per cent.

The absolute error brackets for the cross sections involving He^+ ions are about ± 8 per cent for σ_+ and about ± 11 per cent for σ_-, while the relative accuracies of the cross sections with respect to each other are about ± 5 per cent. The absolute error brackets for the cross sections involving He^{++} ions are about ± 7 per cent for σ_+ and about ± 10 per cent for σ_-, while the relative accuracies are about ± 5 per cent.

CHAPTER VI

COMPARISON WITH AVAILABLE THEORY

A general theoretical treatment[19] of the high-energy ionization process in the Bethe-Born Approximation has shown that for high impact velocity the ionization cross section should be of the general form

$$Q_{n\ell} = \frac{2\pi\ e^4\ c_{n\ell}\ Z_{n\ell}\ Z_i^2}{mv^2\ |E_{n\ell}|} \log_e \left(\frac{2mv^2}{C_{n\ell}}\right) \qquad (6\text{-}1)$$

where e is the electronic charge, $Z_{n\ell}$ is the number of electrons in the $n\ell$ shell of the target atom, each of energy $E_{n\ell}$, Z_i is the charge of the incident ion in units of e, $c_{n\ell}$ is a reduced electron matrix element, $C_{n\ell}$ a quantity related to the energy of an electron in the $n\ell$ shell, m is the electron mass, and v is the collision velocity. Normally σ_i is expected to be essentially equal to $Q_{n\ell}$ for the outermost shell of the target atom. For a given target atom Equation (6-1) can then be written in the form

$$\sigma_i = A \frac{Z_i^2\ M}{E} \log_e (B\ \frac{E}{M}) \qquad (6\text{-}2)$$

where E is the kinetic energy of the incident ion, Z_i is its charge, and M its mass number. The constants:

$$A = \frac{2\pi\ e^4\ c_{n\ell}\ Z_{n\ell}}{2\ m/M_p} \qquad \text{and} \qquad B = \frac{4\ m/M_p}{C_{n\ell}}$$

where M_p is the mass of the proton, are dependent only on properties of the target atom. If A and B are empirically evaluated for a given target atom from experimental data for one incident ion, Equation (6-2) may be used to estimate the ionization cross sections for the same target atom and other incident ions. The cross sections predicted, it must be emphasized, refer only to simple ionization events, as defined in Chapter II, in which the incident ion neither gains nor loses electrons.

Proton data have been fitted by a least squares technique to Equation (6-2) to obtain empirical values of A and B for the target atoms and molecules helium, neon, argon, hydrogen, nitrogen, oxygen, and carbon monoxide.[20]

Incident He^{++} Ions

The ionization cross sections predicted for He^{++} ions incident on helium and hydrogen are presented along with the estimated experimental gross apparent ionization cross sections in Figures 25 and 26 and are labeled "Predicted from Experimental H^+; $Z_i = 2$" in the figures. The procedure by which σ_i was estimated from the experimental σ_+ and σ_- was discussed in Chapter III.

A detailed theoretical calculation of ionization cross sections using the Born approximation for He^{++} ions incident on helium has been made by Mapleton[14] and is presented in Figure 25. Also a similar calculation for He^{++} ions incident on atomic hydrogen has been made by Bates and Griffing.[13] The atomic cross section has been scaled to the molecular cross section by the procedure given in Chapter III and is presented in Figure 26.

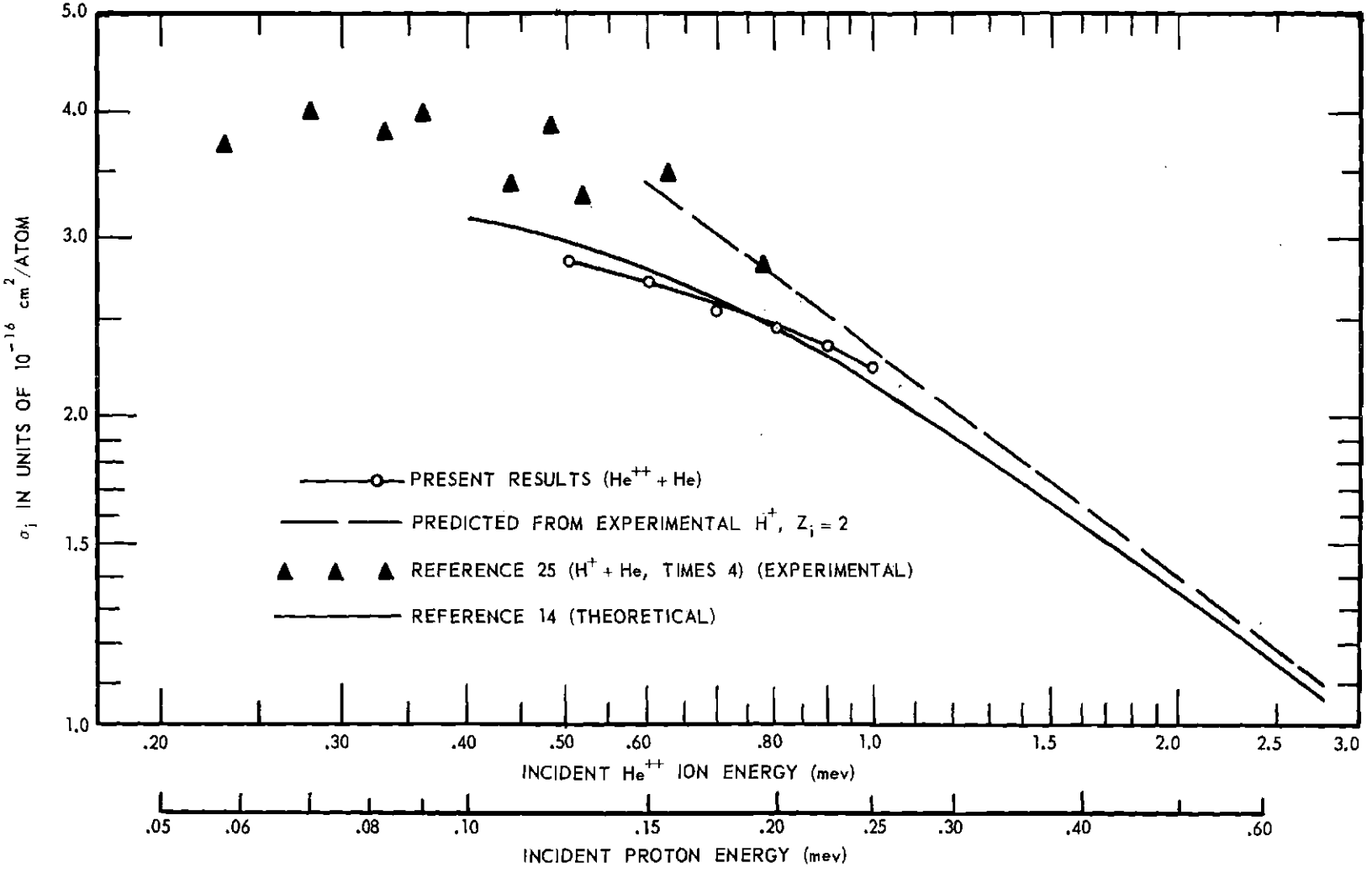

Figure 25. Comparison of Experimental and Theoretical Gross Ionization Cross Sections for He^{++} Ions and Protons of Equal Velocity Incident on Helium.

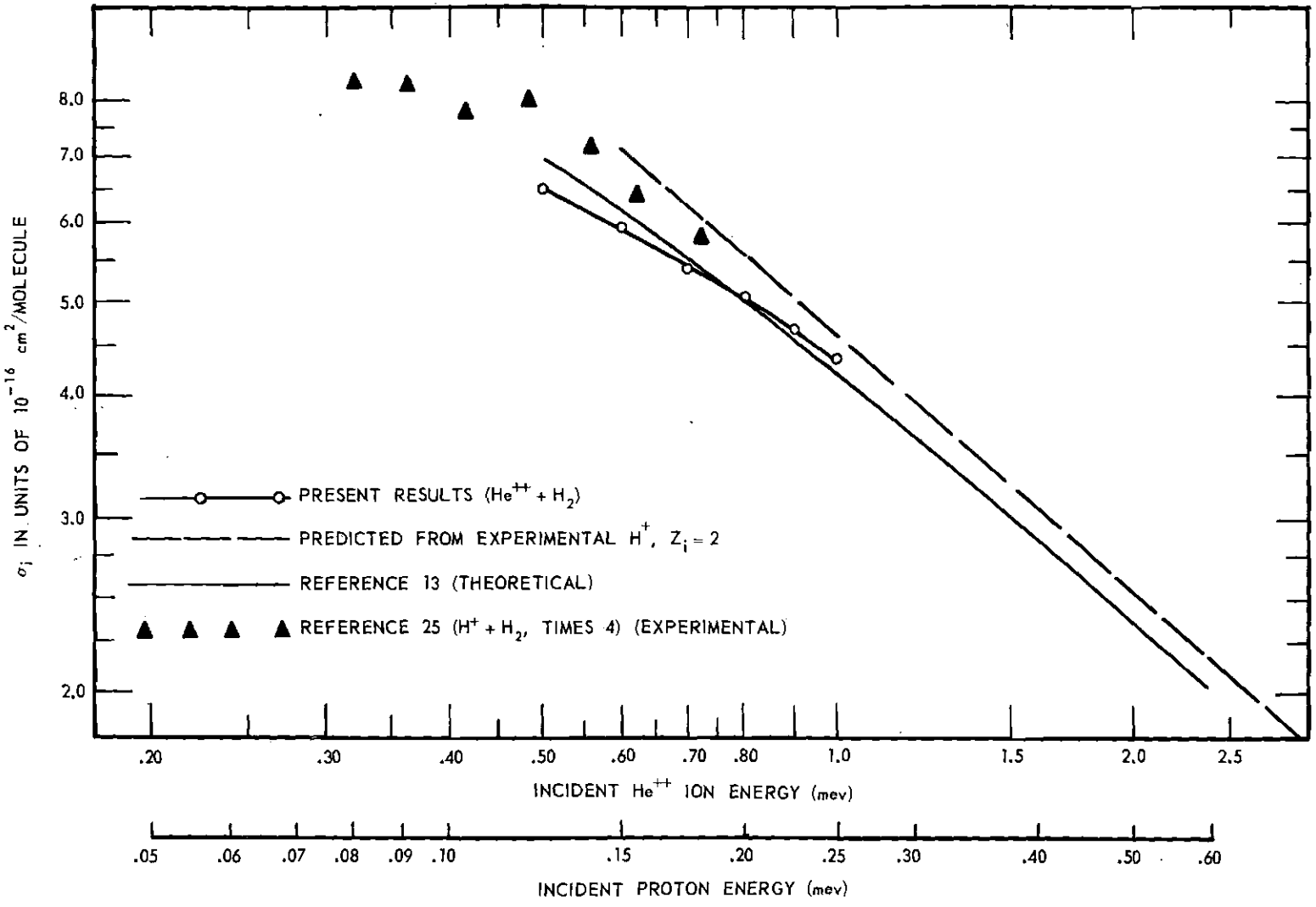

Figure 26. Comparison of Experimental and Theoretical Gross Ionization Cross Sections for He^{++} Ions and Protons of Equal Velocity Incident on Molecular Hydrogen.

The agreement between the present results and the more exact theoretical calculations is excellent while the Bethe-Born calculations using the values of A and B obtained from proton data lie consistently higher by about 10 per cent. This disagreement may have been due to an absolute error in the McLeod gauge that was used for the proton measurements from which the values of A and B were obtained.[17]

Incident He^+ Ions

The relationship between the ionization cross sections for various projectile ions discussed at the first of this chapter should, strictly speaking, apply only to point-charge ions, i.e., to bare nuclei. An incident ion carrying bound electrons might, however, be expected to be equivalent to a partially screened point charge having an "effective" charge Z_i lying somewhere between its actual net charge and its nuclear charge. The value of Z_i for a given ion, and indeed the validity of the whole concept of an effective charge, can for the present be evaluated only by experimental test. The concept will be useful only if Z_i can be shown to be independent of the target atom and of the collision energy, or at least asymptotically so at high energies. If such independence can be established for a given incident ion by measurements taken over a limited energy range, one can use the effective Z_i obtained to extrapolate the measurements to higher energies with Equation (6-2). In addition, one can use the values of A and B for various targets obtained from incident proton measurements to predict the cross sections for other ions of determined effective Z_i on these targets.

Accordingly, a detailed comparison of the present He^+ measurements with earlier proton measurements is presented. Unfortunately the comparison

is not straightforward because for He^+ there are appreciable contributions to the total slow ion production from charge-changing collisions in the energy range investigated, and with presently available information only an estimate can be made of the apparent cross section σ_i for simple ionization. The procedure for arriving at a σ_i for incident He^+ ions is discussed in Chapter II.

The σ_i curves obtained for helium, argon, molecular hydrogen and molecular nitrogen are shown in Figures 27 through 30. A σ_i could not be obtained for the other gases because no charge-changing cross sections are known to have been measured for them to date. Also plotted are the cross sections predicted by Equation (6-2) for $Z_i = 1$, using the values of A and B obtained for these targets from proton measurements,[20] this amounts to just scaling out proton measurements by a factor of four in energy. These cross sections are labeled "Predicted from Experimental H^+; $Z_i = 1$" in the figures.

It is evident that the σ_i curves are indeed nearly parallel to the predicted curves above about 0.60 MeV. They run higher than the predicted curves by a factor of about 1.4 for helium, 1.5 for argon, 1.3 for hydrogen, and 1.5 for nitrogen.

Thus it is shown that the concept of an effective charge Z_i lying between 1 and 2 does indeed have at least qualitative validity for simple ionization by He^+. The value of the effective charge obtained is

$$Z_i \simeq \sqrt{1.4} \simeq 1.2$$

It is noteworthy that this value is materially less than the effective charge of 1.69 deduced from variation calculations of the ground state of

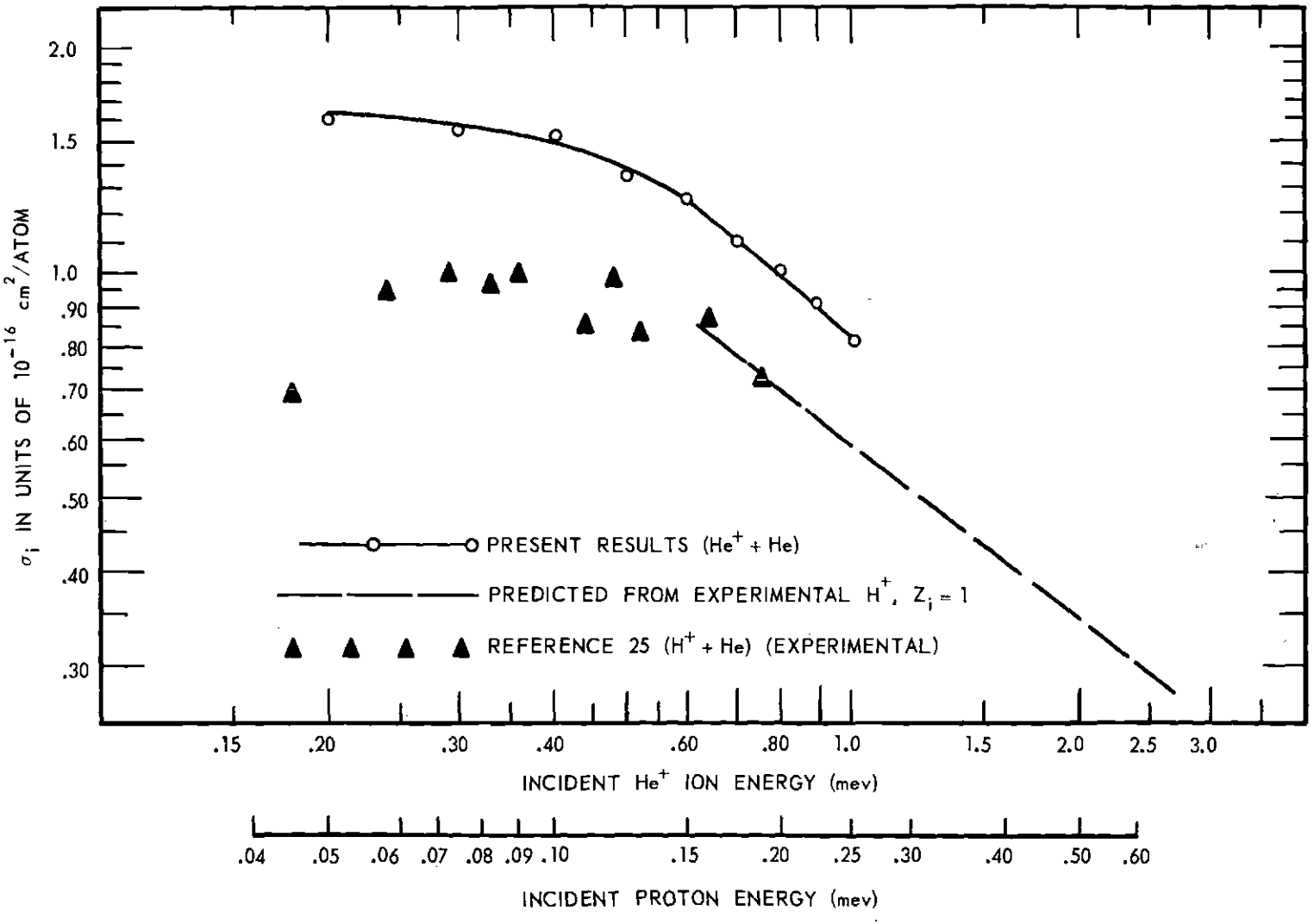

Figure 27. Comparison of Experimental and Theoretical Gross Ionization Cross Sections for He^+ Ions and Protons of Equal Velocity Incident on Helium.

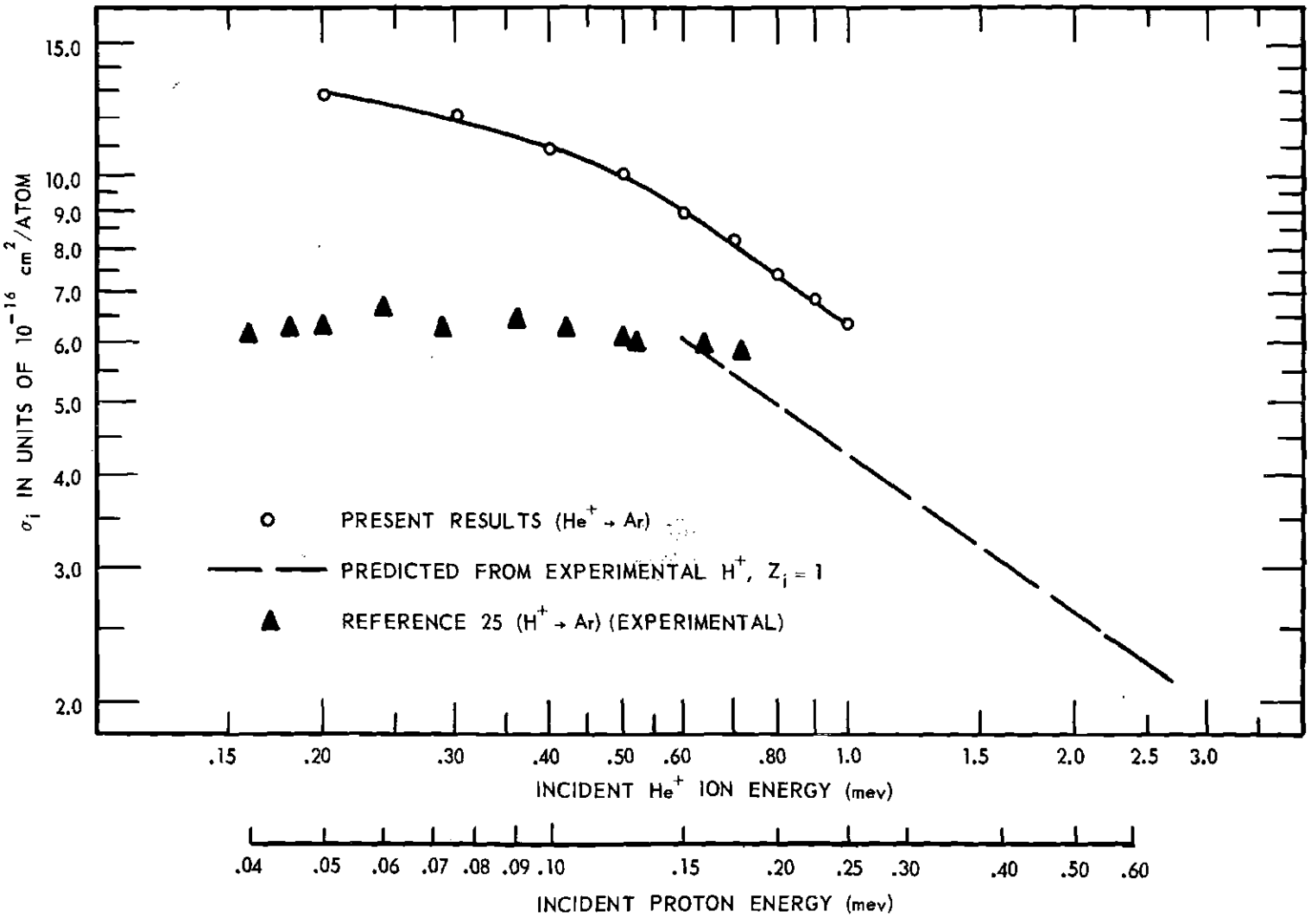

Figure 28. Comparison of Experimental and Theoretical Gross Ionization Cross Sections for He^+ Ions and Protons of Equal Velocity Incident on Argon.

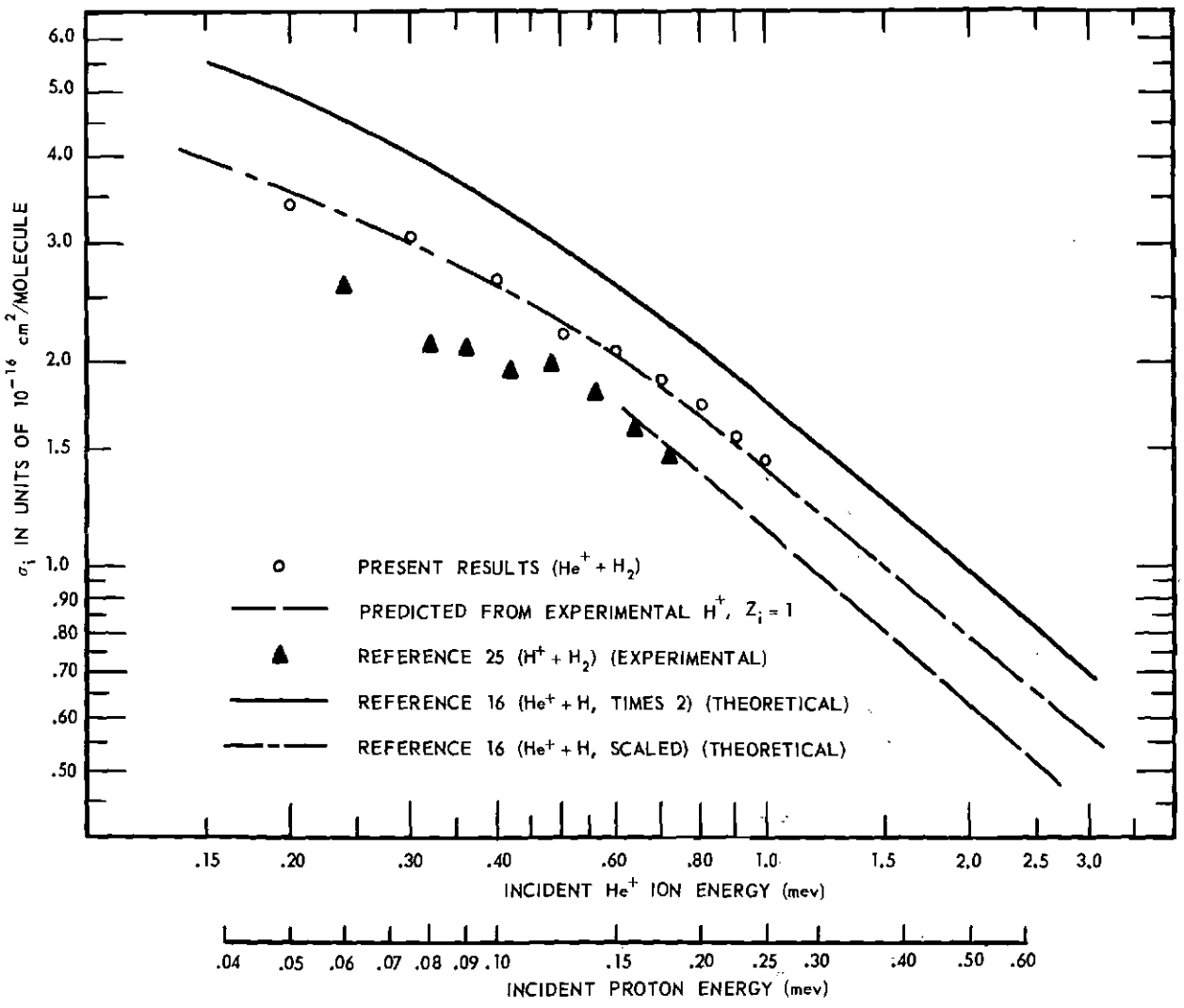

Figure 29. Comparison of Experimental and Theoretical Gross Ionization Cross Sections for He^+ Ions and Protons of Equal Velocity Incident on Molecular Hydrogen.

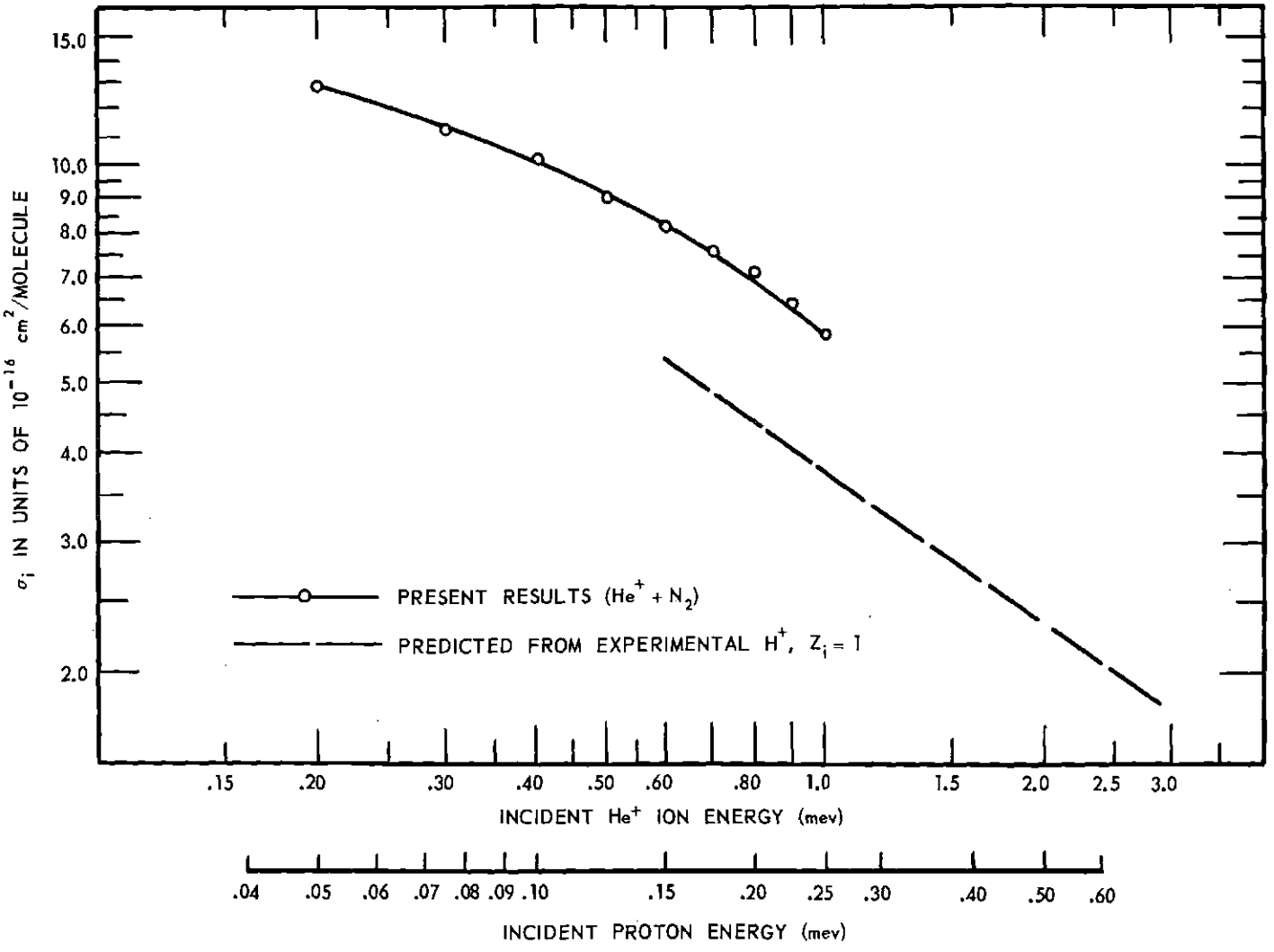

Figure 30. Comparison of Experimental and Theoretical Gross Ionization Cross Sections for He^+ Ions and Protons of Equal Velocity Incident on Molecular Nitrogen.

the neutral helium atom. This difference is not unexpected since the two cases are quite different, and may be most sensitive to quite different spatial regions of the wave function.

A theoretical calculation by Boyd et al. has been made for a bare nucleus plus one electron incident on atomic hydrogen.[16] It was suggested there that a doubling of the atomic cross section would produce the cross section for the molecular structure. This scaling was carried out and is presented in Figure 29. It appears that doubling the atomic cross section is just a first approximation for the molecular cross section. The doubled atomic cross section lies consistantly above the present results. Since this calculation was the same type as that of Bates and Griffing the scaling procedure described in Chapter III was made and the results of it agreed well with present results as is shown in Figure 29.

CHAPTER VII

CONCLUSIONS

The experimental values of the cross sections for the production of slow positive ions for He^+ ions incident on helium, neon, argon, hydrogen, nitrogen, oxygen, and carbon monoxide are presented for comparison in Figure 31, while the cross sections for the production of free electrons for He^+ ions incident on the above mentioned gases are presented for comparison in Figure 32. The energy of the incident particles ranged from 0.133-1.00 MeV.

Theoretical calculations for ionization cross sections using the Born approximation have been made by Mapleton ($He^{++} + He$)[14] and Bates and Griffing ($He^{++} + H$)[13] for point-charge ions, i.e., completely stripped nuclei, and were found to agree well with the present results.

A general theoretical treatment[19] of high energy ionization by Bethe for incident point-charge ions was compared with both helium and hydrogen for incident He^{++} ions. This theory used known experimental proton ionization cross sections to determine needed constants. The agreement between this theory and present results is good. Also the estimated experimental ionization cross sections of several gases by He^+ ions were compared with Bethe's calculations to examine the proposition that the Bethe treatment could be used for the case of an ion carrying bound electrons by using an "effective" charge Z_i lying between the nuclear charge and the actual net charge of the ion. To be a useful concept, the effective charge for a given incident ion must be found to be independent of

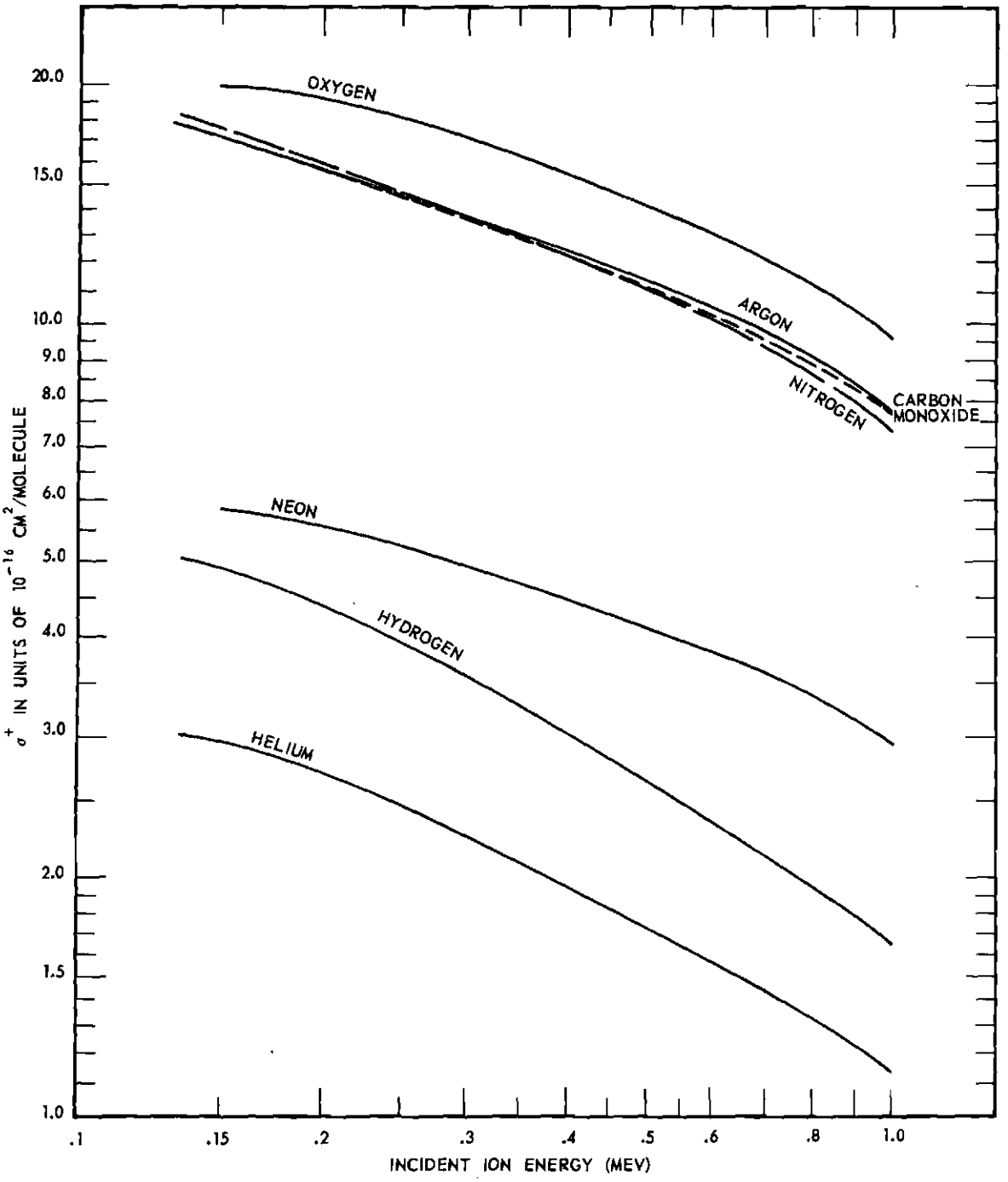

Figure 31. Cross Sections for the Gross Production of Positive Ions by He^+ Ions Incident on Helium, Neon, Argon, Molecular Hydrogen, Molecular Nitrogen, Molecular Oxygen, and Carbon Monoxide.

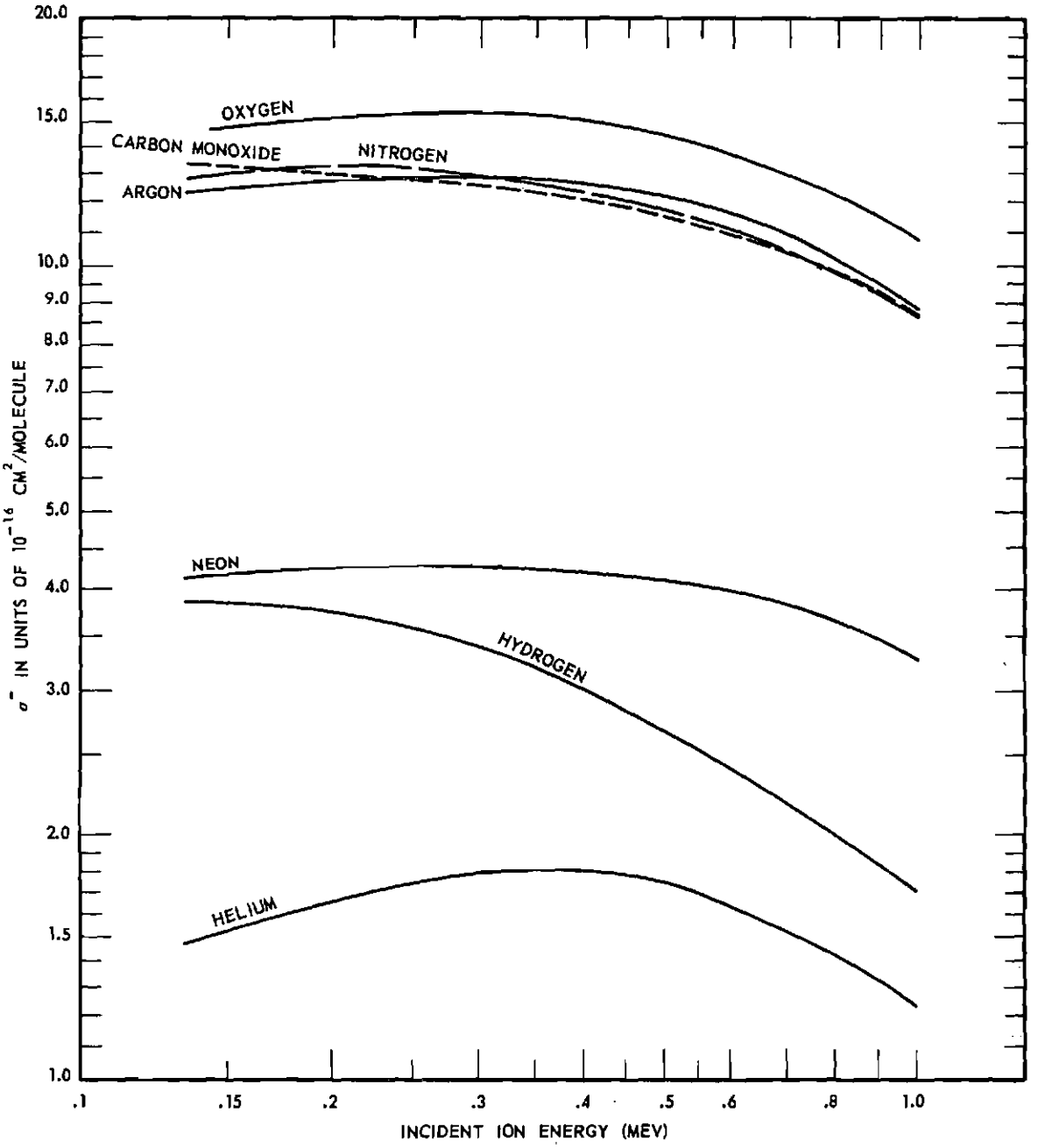

Figure 32. Cross Sections for the Gross Production of Free Electrons by He^+ Ions Incident on Helium, Neon, Argon, Molecular Hydrogen, Molecular Nitrogen, Molecular Oxygen, and Carbon Monoxide.

the target gas and of the incident ion energy. The theoretical calculations referred to here describe only "simple" ionization events in which the incident ion does not gain or lose electrons. Therefore the present experimental data on the total ion and electron production by He^+ had to be corrected for the appreciable contributions from charge-changing events encountered at high energies. With presently available information this correction can be made only approximately, even for those cases where the "stripping" cross section has been measured.[21,24] It was found that the estimated cross section for simple ionization was greater than that for incident protons of the same velocity by a factor that was very nearly independent of energy above 0.6 MeV, and varied only from 1.3 to 1.5 for the four gases hydrogen, helium, argon, and nitrogen. Thus the concept of an effective charge of about 1.2e for He^+ does seem to have at least a qualitative validity. It is noteworthy that this value is appreciably less than the effective charge 1.69e deduced in variation calculations of the ground state wave functions of helium. This difference is not unexpected since the two cases are quite different, and may be most sensitive to quite different spatial regions of the wave function.

A more exact theoretical treatment of He^+ incident on atomic hydrogen has been made by Boyd et al.[16] A doubling of the theoretically determined atomic ionization cross section to obtain the molecular cross section is suspect in that it leads to a cross section higher than the experimentally observed cross section. The scaling procedure described in Chapter III was applied to the theoretical calculations and agreement between the estimated experimental ionization cross section and the scaled theoretical cross section was excellent.

APPENDIX

THE CONCEPT OF THE COLLISION CROSS SECTION

The various reactions which can occur when a beam of monoenergetic particles traverses a gas may be described in terms of reaction cross sections. The following development is only one of several possible presentations of the cross section concept.

Consider a monoenergetic beam of N_o particles per second incident upon a gas whose density is n particles per cubic centimeter. Let N(x) represent the incident beam particles which have not undergone a reaction in traversing the distance x in the gas. The change in the unreacted component of the beam in traversing an infinitesimal distance dx beyond the point P located x units within the gas will be proportional to N(x), n, and dx. Or:

$$-\frac{dN(x)}{dx} \sim N(x)n \qquad \text{(A-1)}$$

where the minus sign indicates a decrease in the number of unreacted particles.

Let the constant of proportionality be represented by σ. Then:

$$-\frac{dN(x)}{dx} = \sigma N(x)n \qquad \text{(A-2)}$$

Integration of Equation (A-2) followed by evaluation of the arbitrary constant yields:

$$N(x) = N_o \varepsilon^{-n\sigma x} \qquad (A-3)$$

A knowledge of N_o, $N(x)$, and n leads to a determination of σ. It will be observed that the proportionality constant σ has the dimensions of $(\text{centimeters})^2$. Therefore σ is called the total reaction cross section for the specific target-projectile combination. It is sometimes convenient to consider the cross section to be an effective projected area of the target particle for the particular reaction or reactions of interest.

If the reactions of interest are those which arise in collision processes, σ may be considered to be the total collision cross section. This total collision cross section may be considered to be made up of the sum of the cross sections for elastic and inelastic collisions for all possible types. Thus:

$$\sigma = \Sigma \sigma_n \qquad (A-4)$$

where σ_o, σ_1, σ_2, σ_3, etc. represent the individual cross sections. In general σ and all of the σ_n are functions of the particle velocity.

To illustrate the use of the concept of collision cross section, consider the following experiment: A homogeneous ion beam is injected into a collision chamber containing target gas atoms at a pressure sufficiently low to insure that only single collisions will occur. The gross cross section for the production of free electrons can be determined by measurement of the electron current.

To construct a model for this experiment let n represent the number of target atoms per unit volume, σ_- the cross section of each target structure for the production of electrons, A the cross sectional area of gas

presented to the incident beam, and N_o the total number of incident particles per second. It follows from the earlier discussion that if we consider an element of the gas of thickness dx the fraction of the target area blocked by the target particles is:

$$f = \frac{A\,\sigma_-\,n\,dx}{A} = \sigma_-\,n\,dx \qquad (A\text{-}5)$$

This result is based on the assumption that the gas pressure is sufficiently low that the shielding of one target atom by another is a negligible effect.

$N_o\,\sigma_-\,n\,dx$ collisions will occur in the length dx. If a sufficiently small number of reactions occur to insure that the incident beam is essentially unaltered in passing through the collision region, $N_o\,\sigma_-\,n\ell$ collisions will occur in the total collision chamber length ℓ. The application of a transverse electric field will result in the collection of a number of electrons which is proportional to the gross electron production cross section σ_-. The total number of electrons collected per unit time under the preceding conditions will be equal to $N_o\,\sigma_-\,n\ell$. The collected electrons will produce a current I^- equal to $N_o\,\sigma_-\,n\ell\,e$, where e denotes the electron charge.

Essentially all of the incident beam current I_i passes through the collision chamber and is collected. It follows that the ratio of the electron current to the total beam current is given by:

$$\frac{I^-}{I_i} = \frac{N_o\,e\,\sigma_-\,n\ell}{N_o\,e} = \sigma_-\,n\ell \qquad (A\text{-}6)$$

Therefore the gross electron production cross section for this special case is:

$$\sigma_- = \left(\frac{1}{n\ell}\right)\left(\frac{I^-}{I_i}\right) \text{ cm}^2/\text{target particle} \qquad \text{(A-7)}$$

A similar analysis applied to a measurement of residual positive ions would lead to the result:

$$\sigma_+ = \left(\frac{1}{n\ell}\right)\left(\frac{I^+}{I_i}\right) \text{ cm}^2/\text{target particle} \qquad \text{(A-8)}$$

BIBLIOGRAPHY

1. H. S. W. Massey and E. H. S. Burhop, Electronic and Ionic Impact Phenomena, London: Oxford University Press, 1956.

2. S. K. Allison, Reviews of Modern Physics, 30, 1137 (1958).

3. S. K. Allison and M. Garcia-Munoz, Atomic and Molecular Processes, Edited by D. R. Bates, New York: Academic Press, Inc., 1962.

4. N. V. Federenko, Soviet Physics Uspekhi, 2, 526 (1959).

5. E. W. McDaniel, Collision Phenomena In Ionized Gases, New York: John Wiley and Sons, Inc., (to be published in 1964).

6. E. H. S. Burhop, Quantum Theory I. Elements, Edited by D. R. Bates, New York: Academic Press, Inc., 1961.

7. M. Gryzinski, Physical Review, 115, 374 (1959).

8. S. Chandrasekhar, Astrophysics Journal, 93, 285 (1941).

9. S. Chandrasekhar and R. E. Williamson, Astrophysics Journal, 93, 305 (1941).

10. R. G. Alsmiller, Oak Ridge National Laboratory Report ORNL-3232 (1962).

11. M. E. Rudd and T. Jorgensen, personal communication (to be printed in the Physical Review).

12. J. B. Hasted, Advances in Electronics and Electron Physics, 13, New York: Academic Press, Inc., 1960.

13. D. R. Bates and G. Griffing, Proceedings of the Physical Society, (London), A66, 961 (1953).

14. R. A. Mapleton, Physical Review, 109, 1166 (1958).

15. G. A. Erskine, Proceedings of the Royal Society (London), A 244, 362 (1954).

16. T. J. M. Boyd, B. L. Moiseiwitsch, and A. L. Stewart, Proceedings of the Physical Society (London), A 70, 110 (1956).

17. J. W. Hooper, Ionization Cross Sections for Protons Incident on Helium, Neon, Argon, Hydrogen, Nitrogen, Oxygen and Carbon Monoxide in the Energy Range 0.15-1.10 MeV, Unpublished Ph.D. Thesis, Atlanta: Georgia Institute of Technology (1961).

18. C. F. Barnett and H. K. Reynolds, Physical Review, 109, 355 (1958).

19. Von H. Bethe, Annals der Physik, 5, 325 (1930).

20. J. W. Hooper, D. S. Harmer, D. W. Martin, and E. W. McDaniel, Physical Review, 125, 2000 (1962).

21. L. I. Pivovar, M. T. Novikov, and V. M. Tubaev, Soviet Physics JETP, 15, 1035 (1962).

22. N. V. Federenko, V. V. Afrosimov, and D. M. Kaminker, Soviet Physics Technical Physics, 1, 1861 (1956).

23. H. B. Gilbody, J. B. Hasted, J. V. Ireland, A. R. Lee, E. W. Thomas, and A. S. Whiteman, personal communication (to be printed in the Proceedings of the Royal Society (London)).

24. L. I. Pivovar, V. M. Tubaev, and M. T. Novikov, Soviet Physics JETP, 14, 20 (1962).

25. V. V. Afrosimoi, R. N. Il'in, and N. V. Federenko, Soviet Physics JETP, 34, 968 (1958).

VITA

Robert Archie Langley was born in Athens, Georgia, on October 21, 1937. He is the son of Archie and Mary Burch Langley. In December of 1959 he was married to Sara Leith Haizlip of Eatonton, Georgia.

He attended public school in Athens, Georgia, and was graduated in 1955. He received the degrees of Bachelor of Science in Physics and Master of Science in Physics in June 1959 and June 1960, respectively, from the Georgia Institute of Technology.

Since 1959 he has been a Graduate Research Assistant at the Engineering Experiment Station. In 1963 he served as a Graduate Instructor of Physics at the Georgia Institute of Technology.